



## Electronic Poster Session - Diffusion & Perfusion

<a href="#">ASL &amp; DCE</a>	3488-3511
<a href="#">ASL &amp; DCE</a>	3512-3535
<a href="#">Diffusion Acquisition, Confounds &amp; Amelioration</a>	3536-3559
<a href="#">Acquisition for Microstructural Imaging, Noise, &amp; Model Fitting</a>	3560-3583
<a href="#">HARDI &amp; Advanced Clinical DWI</a>	3584-3607
<a href="#">Connectivity, Networks, &amp; Kurtosis</a>	3608-3631

---

### ASL & DCE

Click on  to view the abstract pdf and click on  to view the video presentation. (Not all presentations are available.)


Tuesday 8 May 2012

Exhibition Hall

16:00 - 17:00

---

#### Computer #

3488.      1      **Measurement of multi-slice cerebral blood flow with T1-normalized arterial spin labeling MRI using a volume RF labeling coil** 
- Phillip Zhe Sun<sup>1</sup>, Enfeng Wang<sup>1</sup>, Xiaoan Zhang<sup>2</sup>, and Jerry S Cheung<sup>1</sup>
- <sup>1</sup>Department of Radiology, Athinoula A. Martinos Center for Biomedical Imaging, Charlestown, MA, United States, <sup>2</sup>Department of Radiology, 3rd Affiliated Hospital, Zhengzhou University, ZhengZhou, He Nan, China

Arterial spin labeling (ASL) MRI has been increasingly used for examining acute stroke as a research tool. However, CBF calculation requires acquisition of T1app map, which is significantly shorter than the intrinsic T1 map due to concomitant RF irradiation effects. As such, the conventional approach of normalizing with a single T1app value may not be sufficient to characterize regional CBF. We showed that parametric T1app /T1 map remained reasonably homogeneous so that T1app map can be estimated from T1 map, permitting quantitative CBF mapping. The proposed approach has been extended for multi-slice CBF measurement in vivo.

3489.      2      **A setup for continuous arterial spin labeling with a 4**

### **channel radiative labeling coil allowing for high duty cycle labeling at 7T**

Wouter Koning<sup>1</sup>, Johanneke H. Bluemink<sup>1</sup>, Esben Petersen<sup>1</sup>, Alexander Raaijmakers<sup>1</sup>, Anke Henning<sup>2</sup>, Cornelis A.T. van den Berg<sup>1</sup>, Jaco Zwanenburg<sup>1</sup>, Peter Luijten<sup>1</sup>, and Dennis W.J. Klomp<sup>1</sup>

<sup>1</sup>University Medical Center, Utrecht, Netherlands, <sup>2</sup>ETH Zurich, Zurich, Switzerland

A setup is presented for the use of radiative antenna's as external labeling coils for cASL at 7T. Four radiative antenna's attached to a neck pillow filled with heavy water are used to create a B1 field in the neck. This neck pillow can be used in combination with a head coil for labeling during ASL experiments. SAR calculations show that using this setup labeling pulses for cASL can be used with a factor 5.5 longer duration than is allowed with the use of the head coil, while remaining within SAR safety guidelines.

### 3490. 3 **A sequence controlled RF pulse switch at 7T for PASL with an external labeling coil**

Reiner Umathum<sup>1</sup>, and Ann-Kathrin Homagk<sup>1</sup>

<sup>1</sup>German Cancer Research Center, Heidelberg, Germany



A sequence controlled RF pulse switch at 7T for PASL with an external labeling coil R. Umathum, A-K. Homagk Department of Medical Physics in Radiology, German Cancer Research Center (DKFZ), Im Neuenheimer Feld 280, 69120 Heidelberg, Germany Monitoring cerebral blood flow (CBF) using a separate labeling coil for pulsed arterial spin labeling (PASL) usually requires a fully equipped additional RF transmit channel comprising a synthesizer, pulse modulator, power amplifier and a special interface controller. Here we present a solution which is transparent for the scanner hardware, solely controlled by any pulse sequence at run time and which can produce any pulse shape and timing scheme which the ASL imaging sequence is capable of. First results using a water filled head phantom indicate reduced SAR at 300 MHz.

### 3491. 4 **DC-CASL based Quantitative Brain Perfusion Study with a Portable RF Transmitter System**



Xing Lv<sup>1</sup>, Jing Wang<sup>2</sup>, Yudong Zhang<sup>3</sup>, Jue Zhang<sup>1</sup>, Xiaoying Wang<sup>3</sup>, Xiaoping Hu<sup>4</sup>, and Jing Fang<sup>1</sup>

<sup>1</sup>College of Engineering, Peking University, Beijing, Beijing, China, <sup>2</sup>Academy for Advanced Interdisciplinary Studies, Peking University, Beijing, China, <sup>3</sup>Dept. of Radiology, Peking University First Hospital, Beijing, China, <sup>4</sup>Biomedical Imaging Technology Center, Emory University, Atlanta, GA, United States

Among all kinds of arterial spin labeling (ASL) techniques for multi-slice perfusion imaging, Continuous ASL with a separate coil (or Dual-coil CASL) has been proven to have the best SNR with eliminated magnetic transfer interference. However, Most implementations of Dual-Coil CASL(DC-CASL) in previous reports require two independent sets of proton RF channel and amplifier, which are not currently available on most clinical MRI scanners. In this study, a portable RF transmitter, which is based on a single chip microcomputer (SCM)+ Direct Digital Synthesizer (DDS) structure, designed and tested for non-invasive perfusion imaging in clinic. The quantitative CBF measurement results testified the feasibility of this setup. With its high quality imaging, minimized size and low cost, the separated coil based CASL setup may be valuable for further clinical usage.

3492. 5 **Quantitative Mapping of Cerebral Blood Flow with Alternate Ascending/Descending Directional Navigation (ALADDIN)**    
 Sung-Hong Park<sup>1</sup>, Jeffrey W. Barker<sup>1,2</sup>, and Kyongtae Ty Bae<sup>1</sup>  
<sup>1</sup>Radiology, University of Pittsburgh, Pittsburgh, PA, United States, <sup>2</sup>Bioengineering, University of Pittsburgh, Pittsburgh, PA, United States

ALADDIN is a new imaging technique that enables us to perform interslice perfusion-weighted (PW) imaging with no separate preparation pulse. In this article, we investigated the feasibility of quantitative mapping of blood perfusion with ALADDIN at various flip angles. Sensitivity of PW signals kept increasing with flip angle. Centric phase-encode order provided twice higher sensitivity than linear phase-encode order. These experimental results agreed with the simulation results. Cerebral blood flow measured with ALADDIN was close to the values from pulsed arterial spin labeling. The current study helps us to optimize and quantitatively map ALADDIN PW signals.

3493. 6 **Machine learning-based cerebral blood flow quantification for ASL MRI**    
 Ze Wang<sup>1</sup>, Anna Rose Childress<sup>1</sup>, and John A Detre<sup>2</sup>  
<sup>1</sup>Psychiatry, University of Pennsylvania, Philadelphia, Pennsylvania, United States, <sup>2</sup>Neurology, University of Pennsylvania, Philadelphia, Pennsylvania, United States

Arterial spin labeling (ASL) is not stable across time but no one has taken this into account during perfusion quantification. Due to the systematic labeling and control labeling, ASL CBF quantification is a natural two-class data classification process.

Based on this phenomenon, we used a powerful machine learning algorithm, the support vector machine (SVM), to extract the spin labeling function from the ASL data and used it for CBF quantification. The method demonstrated significantly improved temporal SNR and spatial image quality for CBF quantification using normal healthy subjects' data and data from patients with Alzheimer's Disease.

3494. 7 **Optimal kinetic PASL design and CBF estimation with low SNR and Rician noise**  

Li Zhao<sup>1</sup>, and Craig Meyer<sup>1,2</sup>

<sup>1</sup>Biomedical Engineering, University of Virginia, Charlottesville, Virginia, United States, <sup>2</sup>Radiology, University of Virginia, Charlottesville, Virginia, United States

By designing optimal observation times (TI) in dynamic PASL, we can achieve more accurate estimation of CBF. Here, we compare optimal designs for the high/low SNR case, White Gaussian/Rician noise model, and the results from L1/L2 norm estimation. The results show a) optimal sampling design gives accurate estimation, b) low SNR, Rician noise could result biased estimation.

3495. 8 **Improved Temporal Resolution and Reduced Geometric Distortions using Interleaved 3D Spiral Acquisition for Arterial Spin Labeling Imaging**  

Youngkyoo Jung<sup>1,2</sup>, and Megan Johnston<sup>2</sup>

<sup>1</sup>Radiology, Wake Forest School of Medicine, Winston-Salem, NC, United States, <sup>2</sup>Biomedical Engineering, Wake Forest School of Medicine, Winston-Salem, NC, United States

3D ASL imaging provides high SNR benefit over 2D methods. Segmented 3D acquisition methods covering the entire k-space during multiple labeling periods are often preferred to reduce blurring in the slice encoding direction. However, applications of the segmented acquisition are limited to baseline perfusion imaging. We propose an interleaved 3D spiral FLASH imaging method that collects the entire k-space within a single labeling period which offers high temporal resolution, and reduces geometric distortions. We also investigated the trade-off between the number of interleaves and SNR benefit. The proposed method would be beneficial to various ASL applications.



3496. 9 **PASL-like Pseudo Random Amplitude Modulation: measure transit time distribution**  

Xiaowei Zou<sup>1,2</sup>, and Truman R. Brown<sup>2</sup>

<sup>1</sup>Columbia University, New York, NY, United States, <sup>2</sup>Medical

*University of South Carolina, Charleston, SC, United States*



PASL-like Pseudo Random Amplitude Modulation sequence using echo-planar imaging acquisition to measure CBF transit time distribution

3497. 10 **Effects of background suppression on the sensitivity of dual-echo arterial spin labeling MRI for BOLD and CBF signal changes**  

Eidrees Ghariq<sup>1</sup>, Michael A. Chappell<sup>2,3</sup>, Sophie Schmid<sup>1</sup>, Wouter M. Teeuwisse<sup>1</sup>, Mark A. van Buchem<sup>1</sup>, Andrew G. Webb<sup>1</sup>, and Matthias J.P. van Osch<sup>1</sup>

<sup>1</sup>*C.J.Gorter Center for High Field MRI, Leiden University Medical Center, Leiden, Zuid-Holland, Netherlands*, <sup>2</sup>*Institute of Biomedical Engineering, University of Oxford, Oxford, United Kingdom*, <sup>3</sup>*FMRIB Centre, University of Oxford, Oxford, United Kingdom*

Dual-echo arterial spin labeling (DE-ASL) facilitates simultaneous acquisition of BOLD and perfusion-weighted fMRI data. Background suppression (BGS) modules are designed to improve the low intrinsic ASL SNR, but are believed to be undesirable in DE-ASL, because they could decrease BOLD functional sensitivity. In this study, the effects of BGS-pulses on the sensitivity of DE-ASL for BOLD and CBF signal changes were studied. BGS levels of up to 90% were achieved, thereby increasing CBF sensitivity significantly, while loss in BOLD sensitivity remained small, suggesting the possibility of DE-ASL fMRI with BGS.

3498. 11 **In vivo blood T1 measurements at different field strengths: How much do we gain in ASL by moving to higher field strengths?**  

Xingxing ZHANG<sup>1</sup>, Esben T. Petersen<sup>2,3</sup>, Eidrees Ghariq<sup>1</sup>, Jill de Vis<sup>2</sup>, Andrew G. Webb<sup>1</sup>, Wouter M. Teeuwisse<sup>1</sup>, Jeroen Hendrikse<sup>2</sup>, and Matthias J.P. van Osch<sup>1</sup>



<sup>1</sup>*The C.J.Gorter Center for High Field Magnetic Resonance, Leiden University Medical Center, Leiden, Zuid-Holland, Netherlands*, <sup>2</sup>*Department of Radiology, University Medical Center Utrecht, Utrecht, Utrecht, Netherlands*, <sup>3</sup>*Department of Radiotherapy, University Medical Center Utrecht, Utrecht, Utrecht, Netherlands*

Blood T1 is a crucial parameter in the ASL technique, especially for the quantification of CBF. The increase in blood T1 at higher field strengths is one of the main presumed advantages of ASL at higher field MRIs. In this study the blood T1 was measured in the sagittal sinus at three different field strengths: 1.5T, 3T



and 7T. The main findings were that the T1 increased linearly with field strength and that the T1 at 7T (2087ms) was lower than previously reported.

3499. 12 **Revisiting the determination of myocardial perfusion by T<sub>1</sub> based ASL methods applying Look-Locker readout**  
- Thomas Kampf<sup>1</sup>, Xavier Helluy<sup>2</sup>, Christian Herbert Ziener<sup>3</sup>, Peter Michael Jakob<sup>2</sup>, and Wolfgang Rudolf Bauer<sup>4</sup>  
<sup>1</sup>Experimental Physics 5, University of Wuerzburg, Wuerzburg, Bavaria, Germany, <sup>2</sup>Experimental Physics 5, University of Wuerzburg, Germany, <sup>3</sup>Division of Radiology, German Cancer Research Center, Germany, <sup>4</sup>Department of Internal Medicine I, Universitaetsklinikum Wuerzburg, Germany

The effect of the Look-Locker readout scheme on myocardial perfusion measurement applying ASL methods based on T<sub>1</sub> mapping is investigated. Furthermore, the effect of partially inverting the left ventricular blood during the slice selective inversion is considered. Significant influence of each issue on the obtained perfusion is found.

3500. 13 **Rapid estimation of pharmacokinetic parameters can be achieved through a simple vector projection technique applied to DCE-MRI gadolinium uptake curves**  
- Matt N Gwilliam<sup>1</sup>, David J Collins<sup>1</sup>, Martin O Leach<sup>1</sup>, and Matthew R Orton<sup>1</sup>  
<sup>1</sup>CR-UK and EPSRC Cancer Imaging Centre, Institute of Cancer Research, London, United Kingdom

The fitting of pharmacokinetic models to DCE-MRI gadolinium uptake curves is computationally expensive and complicated by several factors including a lack of arterial input function. This work presents a method for determining a simple projection vector, for various pharmacokinetic parameters, that can directly project an uptake curve into PK space. Projection vectors are optimised using a robust fitting algorithm and a training set of uptake curves. The projection vectors are then applied to a set of uptake curves to a test set from a different cohort and good correlation with model fitting techniques is found.

3501. 14 **A Cluster-Based Method for Parametric Maps in Dynamic Contrast-Enhanced -MRI**  
- Patrik Brynolfsson<sup>1</sup>, Anders Garpebring<sup>1</sup>, Thomas Asklund<sup>2</sup>, and Tufve Nyholm<sup>1</sup>  
<sup>1</sup>Dept. of Radiation Sciences, Umeå University, Umeå,

Sweden, <sup>2</sup>Division of Oncology, Dept. of Radiation Sciences, Umeå University, Umeå, Sweden

An alternative method for generation of parametric maps in dynamic contrast-enhanced MRI was investigated on in vivo data. The method is based on clustering of voxels with similar contrast agent kinetics. In this study, the clustering method was compared with a conventional voxel-by-voxel analysis. The results showed that the calculation time was reduced by a factor 8 for a single slice, and parametric maps looked visually similar. However, a correlation analysis revealed that improvements are needed for the cluster-based analysis to reach its full potential.

3502. 15 **Uncertainty in the Pharmacokinetic Analysis of a Modified Reference Region Model Using Dynamic Contrast-Enhanced MRI**  

Yen-Peng Liao<sup>1</sup>, Chi-Jen Chen<sup>1,2</sup>, and Ho-Ling Liu<sup>3</sup>

<sup>1</sup>Department of Medical Imaging, Taipei Medical University - Shuang Ho Hospital, New Taipei City, Taiwan, Taiwan, <sup>2</sup>Department of Medicine, Taipei Medical University, Taipei City, Taiwan, Taiwan, <sup>3</sup>Medical Imaging and Radiological Sciences, Chang Gung University, Taoyuan County, Taiwan, Taiwan

A modified reference region (mRR) model including vascular term for dynamic contrast-enhanced MR imaging (DCE-MRI) can quantify physiological parameters without the need of an arterial input function (AIF). However, inaccurate assumptions of the parameters of a reference region (RR) may induce large estimation error in the quantification of a tissue of interest (TOI). This study aimed to assess the uncertainty in the pharmacokinetic analysis with a mRR model using computer simulations. The results showed estimation errors of [+41.8 to -17.08], [+47.85 to -21.08], and [+37.67 to -24.33] for [-30% to +30%] variations on inaccurate  $K^{trans,RR}$ ,  $v_{e,RR}$  and  $v_{p,RR}$ , respectively.

3503. 16 **Principal components analysis of whole trial onset aligned DCE-MRI gadolinium uptake curves produces metrics that correlate with conventional PK parameter estimates**  

Matt N Gwilliam<sup>1</sup>, David J Collins<sup>1</sup>, Martin O Leach<sup>1</sup>, and Matthew R Orton<sup>1</sup>

<sup>1</sup>CR-UK and EPSRC Cancer Imaging Centre, Institute of Cancer Research, London, United Kingdom

Analysing DCE-MRI Gadolinium uptake curves from a cohort of patients using principal component analysis can produce



metrics that correlate with pharmacokinetic parameters and retain their meaning across datasets implying that treatment effects can be detected. This work demonstrates that these correlations can be improved further by taking into account onset time.

3504. 17 **An Analytical Approach for Quantification and Comparison between Signal Intensity and Longitudinal Relaxation Rate Change ( $\Delta R_1$ ) in MR DCE-T1 Studies** 



Hassan Bagher-Ebadian<sup>1,2</sup>, Siamak P Nejad-Davarani<sup>1,3</sup>, Rajan Jain<sup>4</sup>, Douglas Noll<sup>3</sup>, Quan Jiang<sup>1,2</sup>, Ali Syed Arbab<sup>4</sup>, Tom Mikkelsen<sup>5</sup>, and James R Ewing<sup>1,2</sup>

<sup>1</sup>Neurology, Henry Ford Hospital, Detroit, Michigan, United States, <sup>2</sup>Physics, Oakland University, Rochester, Michigan, United States, <sup>3</sup>Biomedical Engineering, University of Michigan, Ann Arbor, Michigan, United States, <sup>4</sup>Radiology, Henry Ford Hospital, Detroit, Michigan, United States, <sup>5</sup>Neurosurgery, Henry Ford Hospital, Detroit, Michigan, United States

In Dynamic Contrast Enhanced (DCE- MRI) studies, pharmacokinetic models rely on converting the time course of the signal intensity to changes in the longitudinal relaxation rate,  $\Delta R_1(t)$ . However, many researchers employ the normalized Signal Intensity, for quantitative and semi-quantitative DCE analyses instead of  $\Delta R_1(t)$ . In this study, one-dimensional error propagation is applied to the previously described analytical approach in order to investigate the difference between  $\Delta R_1(t)$  and normalized signal intensity profiles. A full analytical methodology is presented for quantifying and comparing the level of agreement in the profiles in both techniques for different levels of contrast enhancement ratios.

3505. 18 **The effect of onset time detection on reproducibility of vascular parameters derived from DCE-MRI**  

Nina Tunariu<sup>1</sup>, David J Collins<sup>1</sup>, Matthew Orton<sup>1</sup>, James A d'Arcy<sup>1</sup>, Christina Messiou<sup>1</sup>, Veronica A Morgan<sup>1</sup>, Sharon L Giles<sup>1</sup>, Catherine J Simpkin<sup>2</sup>, and Nandita M deSouza<sup>1</sup>

<sup>1</sup>CR-UK and EPSRC Cancer Imaging Centre, Institute of Cancer Research and Royal Marsden Hospital, Sutton, London, United Kingdom, <sup>2</sup>CR-UK and EPSRC Cancer Imaging Centre, Institute of Cancer Research and Royal Marsden Hospital, Sutton, United Kingdom

Dynamic contrast enhanced MRI (DCE-MRI) has been successfully used as biomarker of angiogenic activity in preclinical and clinical trials. The time of arrival of the bolus (onset time) definition has a great influence on DCE parameter



estimates and an incorrect onset time can lead to a strong bias. In our experience the automated methods can fail to detect an accurate onset time in cases of tumors that show low contrast uptake, and manual adjustment is essential. This study compares the effect of the onset time as detected using four different methods, on the DCE parameters estimates and their reproducibility.

3506. 19 **Sampling duration in DCE-MRI: In vivo comparison using data acquired within a clinical phase I study** 

Martin Buechert<sup>1</sup>, Henrik Gille<sup>2</sup>, Jan Kuhlmann<sup>3</sup>, and Klaus Mross<sup>4</sup>

<sup>1</sup>MRDAC Magnetic Resonance Development and Application Center, University Medical Center Freiburg, Freiburg, Germany, <sup>2</sup>Pieris AG, Freising, Germany, <sup>3</sup>University Medical Center, Freiburg, Germany, <sup>4</sup>Klinik für Tumorbiologie, Freiburg, Germany



For assessing treatment response DCE-MRI is a valuable tool. Parameters calculated using pharmacokinetic modeling may depend on the sampling duration which equals the number of sampled data points for equally distributed sampling. This was previously investigated by computer simulations but there is limited verification of these findings using real in vivo patient data. This dependency on sampling duration of the  $K_{trans}$ ,  $V_e$  and the fit accuracy were investigated using patient data with a long sampling duration in comparison to an artificial shortened sub set of these data. Results were in agreement with the published simulations.

3507. 20 **Effect on time duration on the precision of pharmacokinetic parameters in DCEMRI**  

Kumar Rajamani<sup>1</sup>, Dattesh Shanbhag<sup>1</sup>, Rakesh Mullick<sup>1</sup>, and Sandeep N Gupta<sup>2</sup>

<sup>1</sup>Medical Image Analysis, GE Global Research, Bangalore, Karnataka, India, <sup>2</sup>Biomedical Image Processing Laboratory, GE Global Research, Niskayuna, NY, United States

We have demonstrated the precision of pharmacokinetic parameters and its effect due to duration of the time-intensity signal. Our results demonstrate that for the prostate case it is preferable to have scan duration of 5 minutes. Scan durations of more than 6 minutes do not generally contribute to any further improvement in the parameters.

3508. 21 **Consistency of permeability measurement using arterial input function and venous output function in DCE-MRI for metastatic brain tumors**  

Yi-Ying Wu<sup>1</sup>, Chen-Hao Wu<sup>1,2</sup>, Chih-Ming Chiang<sup>1</sup>, Chi-Chang Chen<sup>1</sup>, and Jyh-Wen Chai<sup>1</sup>

<sup>1</sup>Department of Radiology, Taichung Veterans General Hospital, Taichung, Taiwan, <sup>2</sup>Institute of Biomedical Engineering, National Taiwan University, Taipei, Taiwan

In DCE-MRI, the venous output function (VOF) from superior sagittal sinus (SSS) is commonly used to replace arterial input function (AIF) to measure permeability of brain lesions. However, there is a lack of comprehensive studies about how to sample the vessel voxels for VOF measurements to achieve a good consistency in quantification of permeability in DCE-MRI. The aim of this study is to investigate the consistency in permeability measurements of metastatic brain tumors using VOF and AIF to analyze DCE-MRI with the commercial-available automatic software.

3509. 22 **Effects of AIF selection and pharmacokinetic model selection on Discrimination of Chronic Infective from Chronic Inflammatory Knee Arthritis using DCE-MRI** 



Prativa Sahoo<sup>1</sup>, Rishi Awasthi<sup>2</sup>, Ram KS Rathore<sup>1</sup>, and Rakesh Kumar Gupta<sup>2</sup>

<sup>1</sup>Mathematics & Statistics, Indian Institute of Technology, Kanpur, Kanpur, Uttar Pradesh, India, <sup>2</sup>Radiodiagnosis, Sanjay Gandhi Post Graduate Institute of Medical Sciences, Lucknow, India, Lucknow, Uttar Pradesh, India

DCE-MRI was performed on 46 patients with 32 patients having Chronic Infective and 14 patients having Chronic Inflammatory Knee Arthritis. Discriminate function analysis was performed to discriminate tubercular and non-tubercular inflammation. For DCE-MRI quantification both local AIF and global AIF was used. Pharmacokinetic analysis was performed using two compartmental and three compartmental model. Our result suggest that Global AIF and Local AIF does not effects the discrimination of tuberculoma from non-tuberculoma however using three compartment model instead of two compartment model significantly improves the discrimination.

3510. 23 **Phase-derived vascular input functions for 2D DCE-MRI of cerebral gliomas: reproducibility and diagnostic value**



Greg O. Cron<sup>1,2</sup>, Thanh B. Nguyen<sup>1,2</sup>, Rebecca E. Thornhill<sup>1,2</sup>, Jean-Francois Mercier<sup>1</sup>, Claire Foottit<sup>1</sup>, Carlos H. Torres<sup>1,2</sup>, Santanu Chakraborty<sup>1,2</sup>, John Woulfe<sup>1,2</sup>, Jean-Michel Caudrelier<sup>1,2</sup>, John Sinclair<sup>1,2</sup>, Matthew J. Hogan<sup>1,2</sup>, Ian Cameron<sup>1,2</sup>, and Mark E. Schweitzer<sup>1,2</sup>

<sup>1</sup>The Ottawa Hospital, Ottawa, ON, Canada, <sup>2</sup>The University of

Ottawa, Ottawa, ON, Canada

For DCE-MRI of cerebral gliomas, temporal resolution can be increased using 2D sequences with limited coverage. However, the resultant saturation and inflow effects distort the measured vascular input function (VIF). A relatively new way to solve this problem is phase-derived VIFs (VIF $\phi$ ). The purpose of this study was to compare the reproducibility and diagnostic value of tracer kinetic parameters (TKPs) calculated with individually-measured VIF $\phi$  and a published population-averaged VIF (VIFpop), in a group of 31 patients. VIF $\phi$  was superior to VIFpop for TKP reproducibility. VIF $\phi$ - and VIFpop- derived TKPs were equally good at distinguishing low- from high- grade tumors.

3511. 24 **Phase-Based Vascular Input Function Validation Using Near-Simultaneous PET-MRI**  

Dominique L. Jennings<sup>1</sup>, Daniel B. Chonde<sup>2</sup>, Jayashree Kalpathy-Cramer<sup>1</sup>, Kim Mouridsen<sup>3</sup>, Gregory Sorensen<sup>1</sup>, Alexander Guimaraes<sup>4</sup>, Bruce Rosen<sup>1</sup>, Tracy Batchelor<sup>5</sup>, Elizabeth R. Gerstner<sup>5</sup>, and Ciprian Catana<sup>1</sup>



<sup>1</sup>Athinoula A. Martinos Center for Biomedical Imaging, Massachusetts General Hospital, Boston, MA, United States, <sup>2</sup>HST, Massachusetts Institute of Technology, Boston, MA, United States, <sup>3</sup>Department of Clinical Medicine, Aarhus University, Aarhus, Denmark, <sup>4</sup>Department of Radiology, Massachusetts General Hospital, Boston, MA, United States, <sup>5</sup>Department of Neurology and Cancer Center, Massachusetts General Hospital, Boston, MA, United States

Phase-based DCE-MRI measurements of the vascular input function are insensitive to common imaging-related artifacts observed in magnitude-based vascular input functions. Here we propose the use of PET-based vascular input functions to evaluate the differences between the two MR-based measurements and relative effects of both on estimates of  $k^{\text{trans}}$ .

## Electronic Poster Session - Diffusion & Perfusion

---

### ASL & DCE

Click on  to view the abstract pdf and click on  to view the video presentation. (Not all presentations are available.)

Tuesday 8 May 2012

Exhibition Hall

17:00 - 18:00

---

## Computer #

3512.

### 1 **Accounting for Pre-Capillary Signal in Arterial Spin Labelling Perfusion**

#### **Measurements**

Michael A Chappell<sup>1,2</sup>, Thomas W Okell<sup>2</sup>,  
Bradley J MacIntosh<sup>3</sup>, Peter Jezzard<sup>2</sup>, and  
Stephen J Payne<sup>1</sup>

<sup>1</sup>*Institute of Biomedical Engineering, University of Oxford, Oxford, United Kingdom,* <sup>2</sup>*FMRIB Centre, University of Oxford, Oxford, United Kingdom,* <sup>3</sup>*Department of Medical Biophysics, University of Toronto, Toronto, Canada*

There a number of sources of signal in Arterial Spin Labelling perfusion measurements. The major components that have been addressed to date are label undergoing exchange in the capillaries from which blood flow measurements can be obtained and that remaining in large arteries. However, it has been proposed that signal in impermeable small arterial vessels before the capillary space may also need to be accounted for. In this work the effects of pre-capillary signal on flow and blood volume estimation using multi-inversion time data and a model-based analysis strategy are examined.

3513.

### 2 **3D High-Resolution Whole-Brain Perfusion Measurement using Pseudo-Continuous ASL at Multiple Post-Labeling Delays**

Qin Qin<sup>1,2</sup>, Alan J Huang<sup>2,3</sup>, Jun Hua<sup>1,2</sup>, Robert Stevens<sup>4</sup>, John E Desmond<sup>5</sup>, and Peter C.M. van Zijl<sup>1,2</sup>

<sup>1</sup>*Department of Radiology, Johns Hopkins University, Baltimore, Maryland, United States,* <sup>2</sup>*Kirby Center, Kennedy Krieger Institute, Baltimore, Maryland, United States,* <sup>3</sup>*Department of Biomedical Engineering, Johns Hopkins University, Baltimore, Maryland, United States,* <sup>4</sup>*Department of Anesthesiology Critical Care Medicine, Johns Hopkins University, Baltimore, Maryland, United States,* <sup>5</sup>*Department of Neurology, Johns Hopkins University, Baltimore, Maryland, United States*

Typically, cerebral blood flow (CBF) measurements using Pseudo-Continuous ASL

(PCASL) are acquired at a single post-labeling delay assuming minimum difference of arterial arrival times (AAT) across regions. We performed 3D high-resolution whole-brain PCASL at multiple post-labeling delays and analyzed the data using a general kinetic model. Both voxel-based and ROI-based fitting results displayed a heterogeneous distribution of AAT in various regions. The PCASL measurements over a series of delays can help estimate CBF and ATT simultaneously, which will improve the accuracy of CBF quantification. Implementation of this approach (15 min) is demonstrated to be feasible on a 3T clinical scanner.

3514.

3

### **Resting State Regional Correlation between FDG-PET and pCASL Perfusion MRI**

Yoon Chung Kim<sup>1</sup>, Yoon-Hee Cha<sup>1</sup>, Shruthi Chakrapani<sup>1</sup>, and Danny JJ Wang<sup>1</sup>

<sup>1</sup>University of California, Los Angeles, CA, United States

Perfusion is normally coupled to metabolism and neural function, and correlations of those for each brain region would be useful in interpreting future studies for investigating normal brain function or a diseased state. However, existing studies comparing ASL and FDG-PET are limited by small sample size. Thus, we performed a systematic evaluation of resting pseudo-continuous ASL (pCASL) and 18FDG-PET on 19 healthy subjects to determine the correlation between perfusion and FDG-PET CMRglu measurements across different brain regions. Our study showed that there is generally a good correlation between ASL CBF and PET CMRglu across pixels in the group mean images whereas the correlation of mean CBF and CMRglu values across 19 subjects is intermediate. We also found that metabolism of caudate and putamen is significantly higher relative to perfusion rate, consistent with an earlier report. While susceptibility effects and ROI size differences may to a certain degree account for the observed regional variations, the biophysical mechanism underlying the coupling and uncoupling of glucose metabolism and perfusion across brain regions warrants further investigation.

3515.

4

### **Hippocampal Longitudinal Sub-region**

## Perfusion Can Be Reliably Measured Using ASL

Xiufeng Li<sup>1</sup>, Jeffrey S. Spence<sup>2,3</sup>, Subhendra N. Sarkar<sup>4</sup>, David E. Purdy<sup>5</sup>, Gregory J. Metzger<sup>1</sup>, Robert W. Haley<sup>3</sup>, and Richard W. Briggs<sup>3,6</sup>

<sup>1</sup>Center for Magnetic Resonance Research, University of Minnesota, Minneapolis, MN, United States, <sup>2</sup>Clinical Sciences, UT Southwestern Medical Center, Dallas, TX, United States, <sup>3</sup>Internal Medicine, UT Southwestern Medical Center, Dallas, TX, United States, <sup>4</sup>Radiology, Harvard Med. School, Beth Israel Deaconess Med. Ctr., Boston, MA, United States, <sup>5</sup>Siemens Healthcare, Malvern, PA, United States, <sup>6</sup>Radiology, UT Southwestern Medical Center, Dallas, TX, United States

Measuring hippocampal longitudinal sub-region perfusion has significant clinical relevance, with potential for better diagnosis and understanding of healthy and pathological hippocampal physiology. To evaluate the reliability of measuring hippocampal longitudinal sub-region perfusion using arterial spin labeling (ASL) imaging, measurement errors due to both random spatial noise and temporal physiological noise in OPTIMAL FAIR ASL studies of rCBF were evaluated. Results indicate that hippocampal longitudinal sub-region perfusion can be reliably measured using ASL imaging.

3516.

## 5 Efficiency and Reliability of Vessel Encoding PCASL

Rui Wang<sup>1</sup>, Zhentao Zuo<sup>1</sup>, Rong Xue<sup>1</sup>, Yan Zhuo<sup>1</sup>, and Danny JJ Wang<sup>2</sup>

<sup>1</sup>State Key Lab of Brain and Cognitive Science, Beijing MRI Center for Brain Research, Institute of Biophysics, Chinese Academy of Sciences, Beijing, China, <sup>2</sup>Neurology, UCLA, Los Angeles, CA, United States

The goal of this study was to estimate the labeling efficiency and longitudinal reliability of vessel encoding pseudo-continuous ASL (VE-PCASL) for the 3 main feeding arteries at 3T, utilizing phase-contrast (PC) MRI as the reference standard. We calculated the global labeling efficiency and those of the right internal carotid (R), left internal carotid (L), and basilar artery (B) of VE-PCASL. Our results demonstrated that the labeling efficiency of VE-

PCASL is reproducible and is not sensitive to labeling locations. However, the labeling efficiency of B was lower than that of the carotid arteries.

3517.

6 **Comparison of regional perfusion imaging between planning-free vessel-encoded and super-selective pseudo-continuous arterial spin labeling MRI**  



Nolan S. Hartkamp<sup>1</sup>, Michael Helle<sup>2,3</sup>, Reinoud P.H. Bokkers<sup>1</sup>, Jeroen Hendrikse<sup>1</sup>, and Matthias J.P. van Osch<sup>4</sup>

<sup>1</sup>Department of Radiology, University Medical Center Utrecht, Utrecht, Netherlands, <sup>2</sup>Institute of Neuroradiology, Christian-Albrechts-Universität, Kiel, Germany, <sup>3</sup>Philips Technologie GmbH, Innovative Technologies, Research Laboratories, Hamburg, Germany, <sup>4</sup>C.J. Gorter Center, Department of Radiology, Leiden University Medical Center, Leiden, Netherlands

The aim of this study was to compare the differences of perfusion territories determined by vessel-encoded and super-selective pseudo-continuous arterial spin labeling MRI. Cases are presented to illustrate the capability of either technique to determine correct perfusion territories in vascular variations and mixed perfusion areas. The results of this study show that perfusion territories of vessel-encoded and super-selective p-CASL RPI agree reasonably well. Vessel encoded ASL however fails to detect mixed perfusion areas, which leads to erroneous boundaries in these areas.

3518.



7 **Comparison of Non-Selective and Vessel-Encoded Pseudocontinuous Arterial Spin Labeling for Cerebral Blood Flow Quantification**  

Thomas W Okell<sup>1</sup>, Michael A Chappell<sup>2</sup>, and Peter Jezzard<sup>1</sup>

<sup>1</sup>FMRIB Centre, Department of Clinical Neurosciences, University of Oxford, Oxford, Oxfordshire, United Kingdom, <sup>2</sup>Institute of Biomedical Engineering, Department of Engineering, University of Oxford, Oxford, Oxfordshire, United Kingdom

Quantification of cerebral blood flow (CBF) may be confounded in brain regions fed by multiple



arteries with different transit delays, as may be the case in patients with significant collateral flow. Vessel-encoded pseudocontinuous arterial spin labeling (VEPCASL) generates artery specific perfusion maps, allowing the fitting of a kinetic model to each arterial component separately. Here we compare CBF quantification and signal-to-noise ratio (SNR) using VEPCASL to conventional PCASL in healthy volunteers. Despite reduced SNR, the CBF estimates from VEPCASL were comparable to those from PCASL. Therefore VEPCASL may improve CBF quantification in cases of mixed blood supply.

3519.

8

### **Quantitative Assessment of collaterals from External Carotid Artery with Modified Vessel Encoded Arterial Spin Labeling**

Yi Dang<sup>1</sup>, Bing Wu<sup>2</sup>, Ying Sun<sup>3</sup>, Dapeng Mo<sup>4</sup>, Xiaoying Wang<sup>1,2</sup>, Jue Zhang<sup>1,3</sup>, and Jing Fang<sup>1,3</sup>

<sup>1</sup>Academy for Advanced Interdisciplinary Studies, Peking University, Beijing, China, <sup>2</sup>Dept. of Radiology, Peking University First Hospital, Beijing, China, <sup>3</sup>College of Engineering, Peking University, Beijing, China, <sup>4</sup>Dept. of Neurosurgery, Peking University First Hospital, Beijing, China

The contribution of collaterals from internal carotid can be assessed by depicting of vascular perfusion territories using arterial spin labeling. But so far there is no method available to evaluate the collateral perfusion territory from external carotid in MR. In this study, we present a new labeling scheme on the basis of the vessel-encoded arterial spin labeling to quantitatively assess collaterals from external carotid. The results demonstrate that the proposed method is able to visualize the perfusion territory of ECA to depict the status of collateral circulation and can be used as a promising tool to assess cerebrovascular surgery.

3520.

9

### **Regional Reduction in Cerebral Blood Flow in Patients with Heart Failure**

Rajesh Kumar<sup>1</sup>, Mary A Woo<sup>2</sup>, Danny JJ Wang<sup>3</sup>, Paul M Macey<sup>2</sup>, Jennifer A Ogren<sup>2</sup>, Gregg C Fonarow<sup>4</sup>, and Ronald M Harper<sup>1</sup>

<sup>1</sup>Neurobiology, University of California at Los

Angeles, Los Angeles, CA, United States, <sup>2</sup>UCLA School of Nursing, University of California at Los Angeles, Los Angeles, CA, United States, <sup>3</sup>Neurology, University of California at Los Angeles, Los Angeles, CA, United States, <sup>4</sup>Cardiology, University of California at Los Angeles, Los Angeles, CA, United States

Heart failure (HF) patients show brain injury in autonomic, neuropsychological, and cognitive regulatory sites, possibly resulting from localized hemodynamic alterations; however, regional cerebral blood flow (CBF) activity in those areas is unknown. We used non-invasive arterial spin labeling (ASL) procedures to assess regional CBF changes in HF subjects over controls. Multiple localized brain sites in HF, including frontal, parietal, and temporal regions, basal-ganglia, limbic, brainstem, and cerebellar areas showed reduced CBF, compared to controls. Regionally reduced CBF may stem from initial injury to midline medullary raphe regulatory sites, which cascades to modify vascular supply to more-rostral and cerebellar areas.

3521.

10

**Evaluating transit time and cerebral blood flow estimates in pulsed arterial spin labeling data among patients with carotid stenoses**  

Bradley J MacIntosh<sup>1,2</sup>, Manus J Donahue<sup>3</sup>, Michael A Chappell<sup>4</sup>, David E Crane<sup>1</sup>, and Peter Jezzard<sup>5</sup>

<sup>1</sup>Imaging Research, Sunnybrook Research Institute, Toronto, ONTARIO, Canada, <sup>2</sup>Medical Biophysics, University of Toronto, Toronto, ON, Canada, <sup>3</sup>Radiology, Vanderbilt University School of Medicine, <sup>4</sup>Institute of Biomedical Engineering, University of Oxford, <sup>5</sup>Clinical Neurology, University of Oxford

Arterial spin labeling can be used to study stroke and other cerebrovascular diseases. Using multiple inflow ASL (i.e. post-label delays), it is possible to estimate cerebral blood flow (CBF) and other relevant parameters like arterial transit time (ATT). We develop a metric to determine the proportion of voxels whose ASL model fit produces significant estimates of CBF and ATT. Participants had a range of carotid artery disease of which some went on to

have a carotid endarterectomy (CEA). Fewer significant CBF voxels were detected in the hemisphere with greater stenosis and among individuals went for CEA surgery.

3522.

11 **Intra-scan reproducibility of white matter perfusion in dementia using pseudo-continuous arterial spin labeling**  

Henri JMM Mutsaerts<sup>1</sup>, Dennis FR Heijtel<sup>1</sup>, Charles BLM Majoie<sup>1</sup>, Edo Richard<sup>2</sup>, and Aart J Nederveen<sup>1</sup>

<sup>1</sup>Radiology, Academic Medical Center, Amsterdam, North-Holland, Netherlands, <sup>2</sup>Neurology, Academic Medical Center, Amsterdam, North-Holland, Netherlands

The present data of 34 patients with varying degrees of dementia suggest that total WM perfusion can be obtained from relatively short scantimes (2 min.) using p-CASL with background suppression. Rather than disregarding WM perfusion data because of too low SNR for voxel-wise analyses, this data encourages to analyze the whole WM perfusion as potential extra marker. This could be a clinically relevant marker as WM degradation is involved in, and may even be the onset of, many neurological disorders.

3523.

12 **Perfusion-based functional connectivity mapping of stroke: an arterial spin labeling fMRI study**  

Iris Asllani<sup>1</sup>, Christian Habeck<sup>2</sup>, Ronald Lazar<sup>2</sup>, and Randolph Marshall<sup>2</sup>



<sup>1</sup>Columbia Universtiy, New York, NY, United States, <sup>2</sup>Columbia Universtiy

One of the most significant challenges in stroke neurology is predicting outcomes. While fMRI has played a key role in our understanding of how stroke affects brain function and cognition, translation of imaging data into clinically useful outcomes has been largely ineffectual. This is mainly due to inherent limitations of task-based BOLD fMRI and to a lack of integration of imaging data with other physiological variables. In this study we address these shortcomings by: 1) Acquiring resting functional connectivity networks of cerebral blood flow (CBF) using arterial spin labeling (ASL) perfusion fMRI. 2)

Assessing how focal injury affects the integrity of these networks. 3) Investigating the relationship between these networks and other physiological correlates of disease. We focus on carotid occlusive disease as an ideal model for testing perfusion based functional networks. We plan to use tissue specific ASL fMRI to identify perfusion resting state functional networks (pRFNs) in patients with carotid occlusive disease and healthy controls. Our primary goal is to assess how pRFNs are affected by infarction, hypoperfusion, functional state, and collateral flow.

3524.

13

**A generalized methodology for detection of vascular input function with dynamic contrast enhanced perfusion data**  



Dattesh D Shanbhag<sup>1</sup>, Sandeep N Gupta<sup>2</sup>, Kumar T Rajamani<sup>1</sup>, Yingxuan Zhu<sup>3</sup>, and Rakesh Mullick<sup>4</sup>

<sup>1</sup>Medical Image Analysis Laboratory, GE Global Research, Bangalore, Karnataka, India, <sup>2</sup>Biomedical Image Processing Laboratory, GE Global Research, Niskayuna, NY, United States, <sup>3</sup>Image Analytics Laboratory, GE Global Research, Niskayuna, NY, United States, <sup>4</sup>GE Global Research, Biosignatures & Signal Processing, Bangalore, Karnataka, India

A completely automated and generalized methodology for detection of vascular input functions with dynamic contrast enhancement data is presented. The technique is demonstrated for brain and prostate DCE data with excellent correlation ( $\sim 0.97$ ) between manually defined VIF and that detected using automated method. The method provides consistent and reliable VIF well suited to anatomy being studied: in brain (sagittal sinus) and in prostate (femoral artery)

3525.

14

**An Automatic Computation Tool for the Estimation of B1-Corrected Pharmacokinetic Parameters**  

Robert Merwa<sup>1</sup>, and Gernot Reishofer<sup>2</sup>

<sup>1</sup>Medical Engineering, Upper Austria University of Applied Sciences, Linz, Austria, <sup>2</sup>Department of Radiology, Medical University of Graz, Graz, Austria

DCE T1-weighted MRI provides a technique for the determination of human tissue parameters. For field strength above 1.5 T B1-inhomogeneities occur which produce considerable intensity variations and the estimation of these tissue parameters fails. In order to tackle this challenge a huge amount of images and complex mathematical calculations are used hence the manual handling is pretty difficult and not fail-safe. The aim of this work was to develop a software package for the automatic calculation of the (a) T1-relaxation time, (b) concentration of the contrast agent, (c) AIF in a major artery and (d) tissue parameters for defined regions.

3526.

15

### **Quantification of contrast agent in human brain using quantitative susceptibility mapping**

Tian Liu<sup>1</sup>, Yinghua Ma<sup>2</sup>, Min Lou<sup>3</sup>, Timothy Vartanian<sup>2</sup>, and Yi Wang<sup>4</sup>

<sup>1</sup>MedImageMetric LLC, New York, NY, United States, <sup>2</sup>Neuroscience and Neurology, Weill Cornell Medical College, New York, New York, United States, <sup>3</sup>Neurology, The Second Affiliated Hospital, Zhejiang University School of Medicine, Hang Zhou, Zhe Jiang, China, <sup>4</sup>Radiology, Weill Cornell Medical College, New York, New York, United States

In vivo quantification of contrast agent using T1/T2\* based methods are subject to large errors due to quenching effects. On the other hand, superparamagnetic iron oxide or gadolinium based contrast agents are highly paramagnetic, making them ideal candidates for quantitative susceptibility mapping. In this study, we demonstrated the feasibility of using QSM for the investigation of vasculature in the human brain tumor.

3527.

16

### **A Method of Reducing Fat-Caused Bias in DCE-MRI Perfusion Measurement**

Su-Chin Chiu<sup>1</sup>, Chun-Jung Juan<sup>2</sup>, Hsiao-Wen Chung<sup>1</sup>, Cheng-Chieh Cheng<sup>1</sup>, Hing-Chiu Chang<sup>3</sup>, Cheng-Yu Chen<sup>2</sup>, and Guo-Shu Huang<sup>2</sup>

<sup>1</sup>Biomedical Electronics and Bioinformatics, National Taiwan University, Taipei, Taiwan, <sup>2</sup>Radiology, Tri-Service General Hospital, Taiwan, <sup>3</sup>GE Healthcare, Taiwan

The effects of fat saturation on quantitative perfusion measurements using dynamic contrast-enhanced (DCE) in parotid glands have been proved. In this study, it is proposed to select a pre-contrast baseline of low-fat tissue to reduce the effect, which is effective in reducing bias from fat content in DCE-MRI of the parotid gland. The disagreements between perfusion measurements with and without fat saturation scan are reduced to the level without statistical significance ( $p > 0.05$ ) both in phantom and in vivo experiments.

3528.

17

### **Quantitative contrast media concentration and proton density images**

Federico Pineda<sup>1</sup>, Marko Ivancevic<sup>2</sup>, Gillian Newstead<sup>1</sup>, Hiroyuki Abe<sup>1</sup>, Johannes Buurman<sup>2</sup>, and Gregory Karczmar<sup>1</sup>

<sup>1</sup>University of Chicago, Chicago, IL, United States, <sup>2</sup>Philips Healthcare, Best, Netherlands

Calibration phantoms that can be inserted in a breast coil during a routine DCE-MRI of the breast were developed. These phantoms provide reference signals that can be used to generate quantitative concentration of contrast media and MRI-detectable proton density maps. To date 23 patients have been scanned with these phantoms, peak concentration values suggest a correlation between malignancy and concentration. MRI-detectable proton density may be a novel source of diagnostically useful information. These quantitative images have the potential to provide standardized, quantitative information that is independent of acquisition parameters, which could facilitate comparisons across different scanners and/or institutions.

3529.

18

### **Quantitative Analysis of DCE-MRI Kinetic Parameter Deviation Induced by Dual-flip-angle T1 Mapping in Head and Neck**

Jing Yuan<sup>1</sup>, Steven Kwok Keung Chow<sup>1</sup>, David Ka Kwai Yeung<sup>1</sup>, Anil T Ahuja<sup>1</sup>, and Ann D King<sup>1</sup>

<sup>1</sup>Imaging and Interventional Radiology, The Chinese University of Hong Kong, Shatin, NT, Hong Kong

This study is to quantitatively evaluate the

kinetic parameter estimation deviation with dual-flip-angle (DFA) T1 mapping in head and neck (HN). 23 patients with HN tumors received DCE-MRI. T1 maps were generated based on multiple-flip-angle (MFA) method and DFA combinations.  $k_{ep}$ ,  $K_{trans}$  and  $v_p$  maps based on MFA and DFAs were calculated and compared in primary tumor, salivary gland and muscle. The results showed that DFA-induced T1 deviations could result in significant errors in kinetic parameter estimation, particularly  $K_{trans}$  and  $v_p$ , even with the optimized DFAs. MFA is suggested for accurate pharmacokinetic analysis in HN if scan time permitted.

3530.

19 **High SNR DCE Imaging for Whole-Brain Perfusion Assessment**  

Philippe Gauderon<sup>1,2</sup>, Marina Salluzzi<sup>2,3</sup>, Michel Louis Lauzon<sup>2,3</sup>, Michael Richard Smith<sup>1,4</sup>, and Richard Frayne<sup>2,3</sup>

<sup>1</sup>Biomedical Engineering, University of Calgary, Calgary, Alberta, Canada, <sup>2</sup>Seaman Family MR Research Centre, Calgary, Alberta, Canada, <sup>3</sup>Radiology, University of Calgary, Calgary, Alberta, Canada, <sup>4</sup>Electrical and Computer Engineering, University of Calgary, Calgary, Alberta, Canada

A fast 3D SPGR sequence is suitable for dynamic contrast enhanced (DCE) cerebral perfusion imaging is demonstrated. As a proof of concept, the investigation validated the suitability of the imaging sequence for quantitative perfusion imaging using a static phantom. Perfusion maps generated from initial in vivo acquisitions were in agreement with literature values. The main shortcoming of the sequence was the low contrast-to-noise ratio (CNR) in cerebral tissue, though this concern was somewhat mitigated by increasing TR and using other approaches to preserve temporal resolution.

3531.

20 **DCE-MRI in Endometrial Carcinomas**  

Renate Gruner<sup>1,2</sup>, Ingrid Salvesen Haldorsen<sup>1</sup>, Torfinn Taxt<sup>1,2</sup>, and Helga Salvesen<sup>2,3</sup>

<sup>1</sup>Dept of Radiology, Haukeland University Hospital, Bergen, Bergen, Norway, <sup>2</sup>University of Bergen, Bergen, Bergen, Norway, <sup>3</sup>Dept of Obstetrics and Gynecology, Haukeland



University Hospital, Bergen, Bergen, Norway

The purpose was to explore the feasibility of dynamic contrast enhanced MRI (DCE-MRI) in endometrial carcinomas and investigate possible correlation between perfusion derived parameters and the apparent diffusion coefficient (ADC) estimated from diffusion weighted imaging. Endometrial carcinoma is the most common gynecological malignancy in industrialized countries, and the incidence is increasing. Tracer kinetic modeling was performed using the adiabatic approximation model of Johnson and Wilson (aaJW). The endometrial carcinomas displayed lower post contrast enhancement and faster contrast wash-out compared to normal myometrium. These first results in ten patients show that DCE-MRI acquisition and modeling is highly feasible in endometrial carcinomas.

3532.

21

**Comparison of permeability estimates derived from DCE-MRI and DCE-CT data in a rodent stroke model**  

Andrea Kassner<sup>1,2</sup>, Meah Gao<sup>2</sup>, Jackie Leung<sup>1</sup>, Madison McGregor<sup>2</sup>, Neil Sokol<sup>2</sup>, and David Mikulis<sup>2,3</sup>

<sup>1</sup>Diagnostic Imaging, The Hospital for Sick Children, Toronto, Ontario, Canada, <sup>2</sup>Medical Imaging, University of Toronto, Toronto, Ontario, Canada, <sup>3</sup>Medical Imaging, Toronto Western Hospital, Toronto, Ontario, Canada

Loss of blood-brain barrier (BBB) integrity in acute ischemic stroke is a precursor to hemorrhagic transformation. Dynamic contrast enhanced (DCE) CT and MR imaging can quantify the integrity of the BBB when used with a suitable pharmacokinetic model. We compared DCE-CT and DCE-MRI permeability ratios in a rodent stroke model using the same pharmacokinetic model and determined a statistically significant correlation between the two modalities. The results of this study open up the possibility for multi-modal DCE studies.

3533.

22

**DCE-MRI informs on proteasome activity on apoptosis of CT26 colon cancer by vascular disrupting agent KML001.**  

HyunJin Park<sup>1</sup>, Jin Seo<sup>2</sup>, Young Han Lee<sup>2</sup>, Ho-

Taek Song\*<sup>2</sup>, Chang Hoon Moon<sup>3</sup>, Hee-Soon Lee<sup>3</sup>, Ho Yong Lee<sup>3</sup>, Hee-Jung Cha<sup>4</sup>, and Young Joo Min<sup>3</sup>

<sup>1</sup>Brain Korea 21 Project for Medical Science, Yonsei University, Seoul, Korea, <sup>2</sup>College of Medicine, Yonsei University, Seoul, Korea, <sup>3</sup>Biomedical Research Center, Ulsan University Hospital, Korea, <sup>4</sup>Department of Pathology, Ulsan University Hospital, Korea

Dynamic contrast enhanced MRI (DCE-MRI) technique can provides quantitative information about the tumor vasculature and it has been widely used to evaluate the biological activity of targeted therapy in clinical trials. However, there has been little known about the quantitative imaging validation of proteasome activity driven by vascular disrupting agent (VDA) in a cancer model by MRI. Therefore, we investigated antivasular effects of VDA in CT26 colon cancer xenograft mouse model following treatment with the KML001 by DCE-MRI. Significant decrease ( $p < 0.05$ ) of Kep was observed in post treatment of KML001.

3534.

23

**In-vivo imaging of hind paws micro vessel damage in the STZ-induced diabetes rat using dynamic contrast enhanced-MRI** 



Shigeyoshi Saito<sup>1</sup>, Yuto Kashiwagi<sup>2</sup>, Ryota Ogihara<sup>1</sup>, Akie Sugiura<sup>1</sup>, Takashi Konishi<sup>1</sup>, Shin Takamatsu<sup>1</sup>, Yuuki Takeuchi<sup>1</sup>, Mana Tsugeno<sup>1</sup>, Kohji Abe<sup>2</sup>, and Kenya Murase<sup>1</sup>

<sup>1</sup>Department of Medical Physics and Engineering, Osaka University, Suita, Osaka, Japan, <sup>2</sup>Innovative Drug Discovery Research Laboratories, Shionogi & Co., Ltd, Toyonaka, Osaka, Japan

Hyperglycemia causes damage in the blood vessels and nerves of the body, which in turn develop into the major complications of diabetes. Peripheral neuropathy and peripheral circulatory disorder may induce diabetic foot lesions Our purpose of this study was to assess peripheral micro-vessel damage in streptozotocin (STZ)-induced diabetic rats by using dynamic contrast-enhanced magnetic resonance imaging (DCE-MRI) and histological experiment.

3535.

24

**Pharmacological MRI in mice with the Rapid Steady State T<sub>1</sub>-technique and intraperitoneal contrast agent administration**  

Teodora-Adriana Perles-Barbacaru<sup>1</sup>, Francois Berger<sup>1</sup>, and Hana Lahrech<sup>1</sup>



<sup>1</sup>Grenoble Institute of Neurosciences, INSERM U836, Grenoble, France

The Rapid Steady State T<sub>1</sub> (RSST<sub>1</sub>) MRI technique, previously used with intravenous injections, can be used with intraperitoneal (i.p.) injections of Gd-DOTA to acquire cerebral blood volume fraction (BVf) maps in mice. The longer time window after i.p. administration of Gd-DOTA is used to study the sensitivity of the RSST<sub>1</sub>-technique to BVf changes induced by the vasodilator Acetazolamide. A 20% BVf increase was observed within 10 minutes after Acetazolamide injection confirming the vascular biodistribution of Gd-DOTA and validating the technique. The RSST<sub>1</sub>-technique with i.p. administration of Gd-DOTA can therefore be used for pharmacological MRI experiments in mice.

## Electronic Poster Session - Diffusion & Perfusion

---

### Diffusion Acquisition, Confounds & Amelioration

Click on  to view the abstract pdf and click on  to view the video presentation. (Not all presentations are available.)

Tuesday 8 May 2012

Exhibition Hall

16:00 - 17:00

---

#### Computer #

3536.

25

**Nucleus Size Determination in Q-Space Analysis of Three-Dimensional Cells**  

Gregory S. Duane<sup>1</sup>, Yanwei W. Wang<sup>2</sup>, Blake R. Walters<sup>2</sup>, and Jae K. Kim<sup>2</sup>

<sup>1</sup>Thunder Bay Regional Research Institute, Thunder Bay, ON, Canada, <sup>2</sup>Thunder Bay Regional Research Institute



The impulse-propagator (matrix) method is extended to a three-dimensional idealized cell geometry describing nucleus,

cytoplasm, and extracellular fluid. A basis is constructed, appropriate for the boundary conditions specified on spheres, consisting of spherical Bessel functions of radius multiplied by spherical harmonics in the angular variables. For a PGSE sequence, clear diffraction patterns are obtained for both nucleus and cytoplasm, with cytoplasm dominating the total signal. Results compare favorably with Monte Carlo simulation results. With OGSE, the nuclear diffraction pattern dominates. In either case, vestiges of the diffraction pattern in the total signal could potentially be used to assess nucleus size.

3537. 26 **Rotationally Invariant Gradient Schemes for Diffusion MRI**  

Carl-Fredrik Westin<sup>1</sup>, Ofer Pasternak<sup>1</sup>, and Hans Knutsson<sup>2</sup>  
<sup>1</sup>*Department of Radiology, BWH, Harvard Medical School, Boston, MA, United States,* <sup>2</sup>*Department of Biomedical Engineering, Medical Informatics, Linköping University, Linköping, Sweden*

Minimizing the error propagation that a diffusion MRI gradient scheme introduces is an important task in the design of robust and un-biased experiments. We propose two schemes for the construction of rotationally invariant multiple-shells. The first is a dual frame method that optimizes the rotation invariance of any set of samples. The second uses a subset of the icosahedral set that can intuitively be used for nested rotationally invariant schemes with pre-defined number of samples. Rotationally invariance produces orientationally unbiased estimates and reduces the correlation of the samples, which is an important feature for reconstruction methods such as multiple shells and compressed sensing.

3538. 27 **Multichannel Diffusion MR Image Reconstruction: How to Reduce Elevated Noise Floor and Improve Fiber Orientation Estimation**  

Christophe Lenglet<sup>1</sup>, Stamatios Sotiropoulos<sup>2</sup>, Steen Moeller<sup>1</sup>, Junqian Xu<sup>1</sup>, Edward J Auerbach<sup>1</sup>, Essa Yacoub<sup>1</sup>, David Feinberg<sup>3</sup>, Kawin Setsompop<sup>4</sup>, Lawrence Wald<sup>4</sup>, Tim E Behrens<sup>2</sup>, and Kamil Ugurbil<sup>1</sup>  
<sup>1</sup>*Center for Magnetic Resonance Research, University of Minnesota, Minneapolis, MN, United States,* <sup>2</sup>*Centre for Functional MRI of the Brain, University of Oxford, Oxford, United Kingdom,* <sup>3</sup>*Advanced MRI Technologies, Sebastopol, CA, United States,* <sup>4</sup>*Department of Radiology, Massachusetts General Hospital, Charlestown, MA, United States*

Signal intensity in magnitude MR images follows a Rician distribution when single-channel receiver coils are employed. For multi-channel coil acquisitions, noise properties change, and the observed noise levels depend on the image

reconstruction method used to combine information from different coils. This is problematic for diffusion-weighted MRI, where any artificial elevation of the noise floor limits the ability to properly quantify the signal attenuation and, ultimately, estimate fiber orientation for tractography. We propose to use a multi-channel SENSE1 reconstruction of GRAPPA un-aliased data, which exhibits Rician noise properties, and demonstrate its advantage over the RSoS reconstruction for fiber orientation estimation.

3539. 28 **Mapping complex white matter structures with d-PFG MRI 3D acquisition scheme**  

Michal E Komlosh<sup>1,2</sup>, Evren Ozarslan<sup>1,2</sup>, Martin J Lizak<sup>3</sup>, and Peter J Basser<sup>1</sup>

<sup>1</sup>STBB, PPITS, NICHD, NIH, Bethesda, MD, United States, <sup>2</sup>CNRM, USUHS, Bethesda, MD, United States, <sup>3</sup>NMRF, NINDS, NIH, Bethesda, MD, United States

<sup>1</sup>STBB, PPITS, NICHD, NIH, Bethesda, MD, United States, <sup>2</sup>CNRM, USUHS, Bethesda, MD, United States, <sup>3</sup>NMRF, NINDS, NIH, Bethesda, MD, United States

<sup>1</sup>STBB, PPITS, NICHD, NIH, Bethesda, MD, United States, <sup>2</sup>CNRM, USUHS, Bethesda, MD, United States, <sup>3</sup>NMRF, NINDS, NIH, Bethesda, MD, United States

A novel 3D acquisition scheme was used to map the average axon diameter of a complex white matter structure with double-PFG filtered MRI. The method was tested on a coronal slice of a rat brain where the orientation of white matter within the corpus callosum is known to vary.

3540. 29 **b-value Dependency of DWI Quantitation and Diagnostic Performance in Detecting Malignant Breast Lesions**  

April M Chow<sup>1</sup>, Victor Ai<sup>2</sup>, Polly SY Cheung<sup>3</sup>, Siu Ki Yu<sup>1</sup>, and Gladys G Lo<sup>2</sup>

<sup>1</sup>Medical Physics & Research Department, Hong Kong Sanatorium & Hospital, Happy Valley, Hong Kong SAR, China, <sup>2</sup>Department of Diagnostic and Interventional Radiology, Hong Kong Sanatorium & Hospital, Happy Valley, Hong Kong SAR, China, <sup>3</sup>Breast Care Center, Hong Kong Sanatorium & Hospital, Happy Valley, Hong Kong SAR, China

Diffusion-weighted imaging (DWI) characterizes the random microscopic motion of molecules and enables assessment of tissue microstructure. This technique has been widely used to characterize malignant and benign breast lesions. A number of studies have been reported to optimize b-value for improving the detection of changes in pathologies in various organs. However, study on effect of b-value on DWI quantitation in detecting malignant breast lesion has been limited. In this study, the effect of b-value on the absolute quantitation of ADC and their diagnostic performance in detecting malignant breast lesions was investigated at 3 T. The results showed that the apparent diffusivities generally decreased with b-value in both malignant breast lesions and normal fibroglandular tissue. The diagnostic accuracy of ADC in detecting malignant breast lesions increased with b-value.

3541. 30 **Probing Neural Structure Using Diffusion Spectrum Imaging and Temporal Diffusion Spectroscopy**  

Jun-Cheng Weng<sup>1,2</sup>, Fatima Ali Nasrallah<sup>3</sup>, and Kai-Hsiang Chuang<sup>3</sup>

<sup>1</sup>*School of Medical Imaging and Radiological Sciences, Chung Shan Medical University, Taichung, Taiwan,* <sup>2</sup>*Department of Medical Imaging, Chung Shan Medical University Hospital, Taichung, Taiwan,* <sup>3</sup>*MRI Group, Singapore Bioimaging Consortium, A\*STAR, Singapore, Singapore*

Diffusion MRI is a technique for studying various aspects of microscopic tissue composition and organization in the central nervous system (CNS). The diffusion time is a key parameter to determine restricted diffusion in microstructures and hence the sensitivity of diffusion MRI to different spatial dimensions. However, it is not straightforward to implement pulsed gradient spin echo (PGSE) diffusion experiments with short diffusion times that are needed to highlight structures at microscopic scales. One alternative is to use oscillating gradient spin echo (OGSE) or the so-called temporal diffusion spectroscopy, which allows short diffusion time better than PGSE sequence, to provide a unique way to measure water diffusion. Diffusion spectrum imaging (DSI) is one of the diffusion MRI techniques that can map complex fiber architecture in the brain. We sought to apply OGSE DSI to identify minuscule neuroarchitecture in the brain. By applying oscillating diffusion-sensitive magnetic gradients to tag translational motion of water molecules, 3D probability density function (PDF) of molecular displacement can be reconstructed from the measured OGSE DSI data. For comparison, diffusion tensor images (DTI) of the rat brain were acquired using the OGSE and PGSE sequences. We demonstrate DSI maps with oscillating gradient revealed novel tissue contrast in the rat hippocampus.

3542. 31 **Optimizing diffusion weighting scheme by Cramer-Rao Lower Bound Analysis and Monte Carlo Simulation**  

Yong Wang<sup>1</sup>, and Sheng-Kwei Song<sup>1</sup>

<sup>1</sup>*Radiology, Washington University in St. Louis, Saint Louis, MO, United States*

Diffusion basis spectrum imaging has recently been developed to resolve the crossing fiber and partial volume effects of inflammation or CSF. However, prototype DBSI diffusion scheme has not been optimized. This study employed Cramer-Rao lower bound analysis to compare the precision of DBSI using a multiple-shell scheme vs. the grid scheme. Monte Carlo simulation was employed to examine the effect of signal quality, diffusion weighting strength, and diffusion gradient

distribution on the accuracy and precision of DBSI. We found that grid scheme with higher SNR, stronger diffusion weighting, and optimized diffusion gradient distribution can significantly improve the quality of DBSI solution.

3543. 32 **In vivo High Angular Resolution Diffusion Imaging at 16.4 Tesla**  

Othman I Alomair<sup>1</sup>, Graham J Galloway<sup>1</sup>, Ian M Brereton<sup>1</sup>, Maree Smith<sup>2</sup>, and Nyoman D Kurniawan<sup>1</sup>

<sup>1</sup>Centre for Advanced Imaging, University of Queensland, Brisbane, Queensland, Australia, <sup>2</sup>Pharmacy School, University of Queensland, Brisbane, Queensland, Australia

Segmented echo planar imaging diffusion weighted imaging has been robust in acquiring data at 16.4 Tesla magnetic field with HARDI reconstruction within experimental time frame.

3544. 33 **MR evaluation of internal gradients in porous systems: SE vs DDIF method.**  

Giulia Di Pietro<sup>1,2</sup>, Marco Palombo<sup>2,3</sup>, and Silvia Capuani<sup>2,3</sup>

<sup>1</sup>IIT@Sapienza, Physics Department, Rome, Italy, <sup>2</sup>"Sapienza" University of Rome, Physics Department, Rome, Italy, <sup>3</sup>CNR IPCF UOS Roma, Physics Department, "Sapienza" University of Rome, Rome, Italy

Effective  $G_i$  measured by using Spin-Echo (SE), Diffusion Decay Internal Field (DDIF) and Modified Diffusion Decay Internal Field (DDIF(M)) method for discriminating porous systems characterized by different pores size were compared. The behaviors of  $G_i$  extracted from SE, DDIF and DDIF(M) as a function of beads sizes, show similar trends. However,  $G_i$  values extracted from SE decay better discriminates between different porous systems when compared to  $G_i$  extracted from DDIF and DDIF(M) decays. Finally SE method, unlike DDIF method, can be easily implemented on clinical scanners and requires less time for data acquisition and data processing than DDIF one.

3545. 34 **The Diffusion Sensitivity of Turbo Spin Echo Sequences Significantly Depends on the Relaxation Times and Diffusion Coefficient**  

Matthias Weigel<sup>1</sup>, and Jürgen Hennig<sup>1</sup>

<sup>1</sup>Dept. of Radiology, Medical Physics, University Medical Center Freiburg, Freiburg, Germany

Recent work showed that 'modern' types of turbo spin echo sequences (TSE) using low and varying refocusing flip angles



and high resolution such as SPACE, VISTA, and CUBE have an inherent diffusion sensitivity  $b_{eff}$ , which can generate participating diffusion contrast in the image. The current work demonstrates that these  $b_{eff}$  are not sequence-specific constants, on the contrary, they notably depend on the relaxation times and T2 in particular, as well as on the diffusion coefficient. Thus, TSE inherent diffusion sensitivity significantly depends on the tissue, which is also valid for TSE based preparation schemes such as the superstimulated echo mechanism.

3546. 35 **Image Distortion and Inter-Station Discontinuity Reduction using High Order Eddy Current Correction in Whole Body Diffusion Weighted Imaging**  

Dan Xu<sup>1</sup>, Gaohong Wu<sup>2</sup>, Kenichi Kanda<sup>2</sup>, Joe K. Maier<sup>2</sup>, and Kevin F. King<sup>1</sup>

<sup>1</sup>Applied Science Lab, GE Healthcare, Waukesha, WI, United States, <sup>2</sup>MR Engineering, GE Healthcare, Waukesha, WI, United States

High order eddy currents (HOEC) can cause significant, direction-dependent image distortions and image shape/intensity discontinuities between station boundaries in whole body diffusion weighted imaging (WB-DWI). In this paper, we use a combined prospective and retrospective compensation method to correct HOEC induced distortions. WB-DWI volunteer results show that the method can effectively reduce in-plane distortion, misregistration, and station boundary discontinuities, thus significantly improving WB-DWI image quality.



3547. 36 **Potential Misinterpretation of Diffusion Tensor Imaging Data due to Head Motion**  

A. Alhamud<sup>1</sup>, M Dylan Tisdall<sup>2,3</sup>, Khader M Hasan<sup>4</sup>, André J.W. van der Kouwe<sup>2,3</sup>, and Ernesta M Meintjes<sup>1</sup>



<sup>1</sup>University of Cape Town, Cape Town, WC, South Africa, <sup>2</sup>Athinoula A. Martinos Center for Biomedical Imaging, <sup>3</sup>Department of Radiology, Harvard Medical School, <sup>4</sup>University of Texas Health Science Center, Houston, United States

Previously, we introduced volumetric navigators (3D-EPI) to perform prospective motion correction in diffusion tensor imaging (DTI) that allows real-time tracking of head pose. The navigated diffusion sequence has been further modified to reacquire motion corrupted diffusion volumes during which the motion exceeded a pre-defined threshold. The purpose of this work is to highlight the effect of subject head motion and the effects of retrospective and prospective motion correction with the reacquisition on the diffusion data, in particular, the



fractional anisotropy (FA) of the whole brain-white matter (WM).

3548. 37 **A combined approach for the elimination of partial volume effects in diffusion MRI**    
 Klaus H. Fritzsche<sup>1,2</sup>, Bram Stieltjes<sup>2</sup>, Thomas van Bruggen<sup>2</sup>, Hans-Peter Meinzer<sup>2</sup>, Carl-Fredrik Westin<sup>1</sup>, and Ofer Pasternak<sup>1</sup>  
<sup>1</sup>Laboratory of Mathematics in Imaging, Harvard Medical School, Boston, Massachusetts, United States, <sup>2</sup>German Cancer Research Center, Heidelberg, Germany

Partial volume is a major confounding factor in the analysis of diffusion tensor imaging datasets. The mixing effects of different compartments within each voxel are non-linear, acquisition dependent, and likely to exceed microstructural effects of interest. In this work, we combine two approaches to ameliorate these problems: Free-water elimination that eliminates intra-voxel CSF contamination and partial volume clustering that classifies and probabilistically selects all non-contaminated voxels. We demonstrate the increased sensitivity of this method in a tract specific analysis of the corpus callosum, recognizing abnormalities on a clinical dataset of Alzheimer's disease, compared with matched controls.

3549. 38 **High-Field Compatible Methods for Reduction of Cerebrospinal Fluid Partial Volume Effects in DTI**    
 Corey Allan Baron<sup>1</sup>, and Christian Beaulieu<sup>1</sup>  
<sup>1</sup>Biomedical Engineering, University of Alberta, Edmonton, AB, Canada

Conventional DTI can be impaired by partial volume effects, particularly for brain structures adjacent to cerebrospinal fluid (CSF). We describe two methods of CSF signal reduction that do not increase SAR nor affect scan time: 1) a reduction of repetition time by acquiring DTI data in smaller sets of slices to reduce the signal contributions from long T1 CSF; 2) the application of a small degree of diffusion weighting on the minimal b values to attenuate CSF (i.e. do not acquire b=0 images). The techniques are evaluated using deterministic tractography of the fornix in five individuals.

3550. 39 **Error analysis and correction of ADC measurements for gradient non-linearity**    
 Dariya I. Malyarenko<sup>1</sup>, Brian D. Ross<sup>1</sup>, and Thomas L. Chenevert<sup>1</sup>  
<sup>1</sup>Radiology - MRI, University of Michigan, Ann Arbor, Michigan, United States

Gradient non-linearity leads to spatially-dependent b-values and consequently significant non-uniformity error (~10-20%) in ADC measurements over clinically-relevant FOVs. For quantitative analysis of ADC errors, a gradient correction tensor model of spatially-dependent gradient fields was used. The model included the effect of imaging gradients, gradient cross-terms and their influence in presence of media anisotropy. All-inclusive error analysis allowed finding minimal number of spatial correction terms to achieve sufficient ADC error reduction (by 75-95%) for tissue-like diffusion anisotropy. Simplified ADC correction algorithm is suggested for implementation on MR systems based on known gradient hardware properties

3551. 40 **Straightforward Method to Improve Sensitivity in Diffusion Imaging Studies of Subjects Who Move**  

Joelle E Sarlls<sup>1</sup>, Philip Shaw<sup>2,3</sup>, Nancy E Adleman<sup>4</sup>, and Vinai Rooopchansingh<sup>5</sup>

*<sup>1</sup>NINDS/NIH MRI Research Facility, National Institutes of Health, Bethesda, MD, United States, <sup>2</sup>NIMH, National Institutes of Health, <sup>3</sup>NHGRI, National Institutes of Health, <sup>4</sup>NIMH/Emotion and Development Branch, National Institutes of Health, <sup>5</sup>NIMH/Functional MRI Facility, National Institutes of Health*

A retrospective study of pediatric imaging data revealed widespread corruption of diffusion images due to large head motion. Using an automated real-time software framework, and straightforward calculations in AFNI, diffusion-weighted imaging volumes that have been corrupted by large motions can be detected and reacquired within a scan session. This rapid diffusion QA method provides an efficient way for consistent diffusion data sets to be acquired, with minimal scan time. Reacquiring the corrupted diffusion data avoids potential bias due to removal of variable numbers of corrupted volumes and potentially increases sensitivity to detect change in diffusion properties in populations that tend to move.

3552. 41 **Effects of Diffusion Weighted Image Interpolation for Motion and Distortion Correction on Tensor Statistics**  

Mustafa Okan Irfanoglu<sup>1,2</sup>, Lindsay Walker<sup>1,2</sup>, Raghu Machiraju<sup>3</sup>, and Carlo Pierpaoli<sup>1</sup>

*<sup>1</sup>NIH, NICHD, Bethesda, MD, United States, <sup>2</sup>Center for Neuroscience and Regenerative Medicine, Uniformed Services University of the Health Sciences, Bethesda, MD, United States, <sup>3</sup>Computer Sciences & Engineering, The Ohio State University, Columbus, OH, United States*

Diffusion imaging data generally requires additional postprocessing in order to correct for artifacts and distortions. Typical correction methodologies involve the use of image registration techniques, which employ some form of interpolation to generate the final corrected images. The effects of these interpolation steps have generally been disregarded in the community. In this work, we show that even with the same data and fixed registration correction parameters, the choice of interpolation technique can have a profound effect on the distribution of tensor derived scalar quantities, hence can affect the outcomes of histogram based analysis.

3553. 42 **Automated detection, evaluation and removal of DWI-related artifacts** 

Danilo Scelfo<sup>1</sup>, Laura Biagi<sup>1</sup>, Mauro Costagli<sup>1,2</sup>, and Michela Tosetti<sup>1,2</sup>

<sup>1</sup>IRCCS "Stella Maris" Scientific Institute, Pisa, Italy, Italy, <sup>2</sup>IMAGO7, Pisa, Italy

We proposed algorithm for the automatic detection and removal of diffusion-related artifacts which seems to be a useful tool to be exploited in the normal DW images pre-processing. It allows the user to detect and evaluate potential artifacts and, if required, to remove the volume corresponding to the detected artifact and rearrange the coordinate table of the applied diffusion gradients.

3554. 43 **Using wild bootstrap to evaluate the effect of spatial resolution on MR diffusion parameters**  

Daniel Güllmar<sup>1</sup>, Catharina Lange<sup>1,2</sup>, Christian Ros<sup>1</sup>, Andreas Deistung<sup>1</sup>, and Jürgen R Reichenbach<sup>1</sup>

<sup>1</sup>Medical Physics Group / IDIR I, Jena University Hospital, Jena, Thuringia, Germany, <sup>2</sup>University of Applied Sciences, Jena, Thuringia, Germany

We have used DTI wild bootstrapping method to evaluate different diffusion protocol settings in order to optimize spatial resolution in terms of standard deviation of typical diffusion tensor properties like fractional anisotropy and cone of uncertainty.

3555. 44 **Mask-Based Motion and Eddy-Current Correction of High b-value Diffusion-Weighted Images**  

David Raffelt<sup>1,2</sup>, J-Donald Tournier<sup>1,3</sup>, Olivier Salvado<sup>2</sup>, and Alan Connelly<sup>1,3</sup>

<sup>1</sup>Brain Research Institute, Florey Neuroscience Institutes, Melbourne, VIC, Australia, <sup>2</sup>The Australian E-Health Research

*Centre, CSIRO, Brisbane, QLD, Australia, <sup>3</sup>Department of Medicine, University of Melbourne, Melbourne, VIC, Australia*

Tractography and voxel-based analysis of diffusion-weighted images (DWI) benefit from higher-order models that require the acquisition of a large number of diffusion orientations at high b-values. The associated long scan times increase the likelihood of subject motion. Furthermore, high b-value DWI is also more prone to eddy-current induced distortions. Existing methods to correct motion and eddy-current artefacts are inadequate due to the poor SNR associated with high b-values. We present a robust method to correct motion and eddy-current artefacts in high b-value data. Validation experiments demonstrate that the proposed method can accurately correct  $b=3000\text{s/mm}^2$  data with typical noise levels.

3556. 45 **Effect of Registration on Fractional Anisotropy Values** 



Kurt Hermann Bockhorst<sup>1</sup>, Priya Goel<sup>1</sup>, and Ponnada A Narayana<sup>1</sup>

<sup>1</sup>DII, University of Texas, Houston, Texas, United States

Registration is commonly used during the post processing of medical imaging data. However, the effect of registration on the quantification of imaging metrics as DTI has not been reported recently. The submitted abstract documents a significant decrease of FA values (up to 20%) in the white matter (splenium and genu) of rat brains after registration. We studied this phenomenon with four different types of registration: AIR, FSL, DTI-TK (tensor based) and ANTS. All of these methods caused a significant decrease in FA.

3557. 46 **Diffusion Tensor Uncertainty: Visualization and Similarity Metrics**  

Mustafa Okan Irfanoglu<sup>1,2</sup>, Michael Curry<sup>1</sup>, Evren Özarlan<sup>1,2</sup>, Cheng Guan Koay<sup>1</sup>, Sinisa Pajevic<sup>1</sup>, and Peter J. Basser<sup>1</sup>

<sup>1</sup>NIH, NICHD, Bethesda, MD, United States, <sup>2</sup>Center for Neuroscience and Regenerative Medicine, Uniformed Services University of the Health Sciences, Bethesda, MD, United States

The uncertainty inherent in the estimated diffusion tensors can have profound effects on the analysis outcomes. In this work, we propose a novel method to visualize DTI uncertainty along with similarity metrics that incorporate this information. These metrics can be employed in a variety of applications including tensor field image registration or tensor image segmentation.



3558. 47 **Impact of noise correction on diffusion kurtosis**

**estimation**  

Elodie André<sup>1</sup>, Evelyne Balteau<sup>1</sup>, Christophe Phillips<sup>1</sup>, Ezequiel Farrher<sup>2</sup>, Ivan Maximov<sup>2</sup>, Farida Grinberg<sup>2</sup>, and N. Jon Shah<sup>2,3</sup>

<sup>1</sup>Cyclotron Research Centre, University of Liège, Liège, Belgium, <sup>2</sup>Institute of Neuroscience and Medicine - 4, Forschungszentrum Jülich GmbH, Jülich, Germany, <sup>3</sup>JARA - Faculty of Medicine, RWTH Aachen University, Aachen, Germany

Low SNR is a critical issue in diffusion kurtosis imaging because of the use of high b-values (up to 3000 s mm<sup>-2</sup>). We tested different noise correction methods prior to kurtosis fitting and show that noise correction is a necessary step in kurtosis processing, providing higher tissue contrast and better parameter estimates.

3559. 48 **Local regularization of the diffusion tensor by means of independent component analysis and total variation - application to high resolution DTI**  

Gernot Reishofer<sup>1</sup>, Karl Koschutnig<sup>2</sup>, Christian Langkammer<sup>3</sup>, Stefan Ropele<sup>3</sup>, Stephen Keeling<sup>4</sup>, Robert Merwa<sup>5</sup>, and Franz Ebner<sup>6</sup>



<sup>1</sup>Radiology, Medical University of Graz, Graz, Styria, Austria, <sup>2</sup>Psychology, University of Graz, <sup>3</sup>Neurology, Medical University of Graz, <sup>4</sup>Mathematics and Scientific Computing, University of Graz, <sup>5</sup>Medical Engineering, Upper Austria University of Applied Sciences, <sup>6</sup>Radiology, Medical University of Graz

Advanced scan techniques in diffusion tensor imaging (DTI), such as readout segmented EPI enable high resolution DTI, but suffer from low signal to noise ratio. In this work we present a novel method for the spatially dependent regularization of the diffusion tensor based on independent component analysis and total variation regularization. We demonstrate that the diffusion tensor evaluated from noisy DWI data is successfully denoised, while fine structural details are preserved. This allows for the application of high resolution DTI in a clinically acceptable time.

## Electronic Poster Session - Diffusion & Perfusion

---

### Acquisition for Microstructural Imaging, Noise, & Model Fitting

Click on  to view the abstract pdf and click on  to view the video presentation. (Not all presentations are available.)

Tuesday 8 May 2012

Exhibition Hall

17:00 - 18:00

**Computer  
#**

3560.



25

**Optimal b-Value Range in Diffusion  
Kurtosis Imaging**  Ezequiel Farrher<sup>1</sup>, Farida Grinberg<sup>1</sup>, and N. Jon Shah<sup>1,2</sup>*<sup>1</sup>Institute of Neuroscience and Medicine - 4, Forschungszentrum Juelich, Juelich, Germany, <sup>2</sup>JARA - Faculty of Medicine, RWTH Aachen University, Aachen, Germany*

In the recent years, diffusion kurtosis imaging has become an important method for the quantification of the non-Gaussian diffusion in brain tissue by means of magnetic resonance imaging. In this work we carry out an experimental investigation of the optimal allowed range of b-values according to the type of tissue under examination and an applied set of gradient directions. We examine how the mean-diffusivity and mean-kurtosis maps are influenced by the chosen range of b-values and propose an optimization scheme.







3561.

26

**Gaussian Phase Distribution Approximation  
of the Square Wave Oscillating Gradient  
Spin-Echo (SWOGSE) Diffusion Signal**  Andrada Ianus<sup>1</sup>, Bernard Siow<sup>1</sup>, Hui Zhang<sup>1</sup>, and Daniel C. Alexander<sup>1</sup>*<sup>1</sup>University College London, London, United Kingdom*

This work presents analytical formulae for both free and restricted diffusion NMR signal from a square wave oscillating gradient spin-echo (SWOGSE) sequence. The expressions are computed using the Gaussian Phase Distribution approximation and we demonstrate for cylindrical geometry. The results for different radii, frequencies, and gradient strengths are compared with the values obtained from Monte Carlo diffusion simulation. In all cases the error was less than 3% of the signal and the total computation time was reduced by several orders of magnitude, which enables model fitting applications, e.g. to generate whole brain parameter maps.



3562. 27 **Neurite Density Measured in Human Subject using Hybrid Diffusion Imaging**    
 Shiyang Wang<sup>1,2</sup>, Michael Chopp<sup>1,2</sup>, Siamak Pourabdollah Nejad D.<sup>1</sup>, JiaNi Hu<sup>3</sup>, and Quan Jiang<sup>1,2</sup>  
<sup>1</sup>Neurology, Henry Ford Hospital, Detroit, MI, United States, <sup>2</sup>Physics, Oakland University, Rochester, MI, United States, <sup>3</sup>Radiology, Wayne State University, Detroit, MI, United States
- Neurite density measured in healthy volunteers using hybrid diffusion. Neurite density measured in TBI patient using simultaneous image refocusing sequence combined with hybrid gradient encoding scheme.
3563. 28 **In Vivo Human Brain Measurements of Axon Diameter Distributions in the Corpus Callosum using 300 mT/m Maximum Gradient Strengths**    
 Jennifer A. McNab<sup>1</sup>, Thomas Witzel<sup>1</sup>, Himanshu Bhat<sup>2</sup>, Keith Heberlein<sup>2</sup>, Boris Keil<sup>1</sup>, Julien Cohen-Adad<sup>1</sup>, M. Dylan Tisdall<sup>1</sup>, and Lawrence L. Wald<sup>1,3</sup>  
<sup>1</sup>A.A. Martinos Center for Biomedical Imaging, Radiology, Massachusetts General Hospital, Harvard Medical School, Boston, MA, United States, <sup>2</sup>Erlangen USA Inc., Siemens Medical Solutions, Charlestown, MA, United States, <sup>3</sup>Harvard-MIT Division of Health Sciences and Technology, Massachusetts Institute of Technology, Cambridge, MA, United States
- In this work we use a novel gradient coil AS302 which is part of a new 3T system (MAGNETOM Skyra CONNECTOM, Siemens Healthcare) capable of up to 300 mT/m to measure, in the *in vivo* human brain, the full axon diameter distribution in the corpus callosum as determined by the AxCaliber method.
3564. 29 **Double wave vector diffusion weighting in Wallerian degeneration**  

Martin A. Koch<sup>1,2</sup>, and Jürgen Finsterbusch<sup>1</sup>  
<sup>1</sup>*Systems Neuroscience, Neuroimage Nord, University Medical Center Hamburg-Eppendorf, Hamburg, Germany,* <sup>2</sup>*Institute of Medical Engineering, University of Lübeck, Lübeck, Germany*

Double wave vector diffusion weighting is a new approach for assessing tissue characteristics such as mean pore size and shape: for restricted diffusion the MR signal acquired with two successive diffusion weighting periods may depend on the angle between the two applied gradient directions. At short mixing times, the signal difference between parallel and antiparallel gradient orientations can be related to the mean pore size. It is investigated whether the size estimate derived from this signal difference is sensitive to pathological changes in the tissue microstructure of the corticospinal tracts.

3565.

30

**Diffusion MR Imaging at varying of diffusion time to give more on the heterogeneous porous systems.**  

Marco Palombo<sup>1,2</sup>, Cesare Cametti<sup>1</sup>, Mariella Dentini<sup>3</sup>, and Silvia Capuani<sup>1,2</sup>

<sup>1</sup>*"Sapienza" University of Rome, Physics Department, Rome, Rome, Italy,* <sup>2</sup>*CNR IPCF UOS Roma, Physics Department "Sapienza" University of Rome, Rome, Italy,* <sup>3</sup>*"Sapienza" University of Rome, Department of Chemistry, Rome, Italy*



We introduce a novel imaging method to characterize and to map anomalous diffusion processes of water in heterogeneous systems by means of diffusion weighted NMR techniques at varying of the diffusion time. The approach is based on the theory of the Continuous-Time-Random-Walk and introduces the  $\alpha$  index, which quantify sub-diffusion processes. We present the first  $\alpha$ -map obtained in two controlled porous phantoms characterized by the same void and interconnect size distribution but by different type of porous matrix walls (smooth or rough). Our results show that  $\alpha$ -maps, unlike the conventional MD-maps, are able to discriminate between these two samples.

3566. 31 **AN EFFICIENT PROTOCOL FOR COMPREHENSIVE ASSESSMENT OF WHITE MATTER MICROSTRUCTURE BY COMBINING RELAXATION AND DIFFUSION IN ONE MODEL**  

Silvia De Santis<sup>1</sup>, Tim Vivian-Griffiths<sup>1</sup>, Sonya Bells<sup>1</sup>, Yaniv Assaf<sup>2</sup>, Sean Deoni<sup>3</sup>, and Derek K Jones<sup>1</sup>

<sup>1</sup>*CUBRIC, Cardiff University, Cardiff, United Kingdom*, <sup>2</sup>*Tel Aviv University, Tel Aviv, Israel*, <sup>3</sup>*Brown University, United States*

In this work, we develop an efficient and clinically-applicable protocol that provides comprehensive assessment of WM microstructure, providing not only estimates of FA, but also of the attributes of WM that drive differences in FA. Combining relaxometric and diffusion acquisition maps, the axonal diameter distribution can be obtained with a clinical setup. The resulting protocol comprehensively characterizes WM features (AD, myelination, axon density), overcoming the lack of specificity of DTI measures and thus allowing specific conclusions to be drawn when looking at group differences.

3567. 32 **Investigating tissue microstructure using diffusion MRI: How does the resolution limit of the axon diameter relate to the maximal gradient strength?**  

Markus Nilsson<sup>1</sup>, and Daniel Alexander<sup>2</sup>

<sup>1</sup>*Department of Medical Radiation Physics, Lund University, Lund, Sweden*, <sup>2</sup>*Centre for Medical Image Computing, Department of Computer Science, University College London, London, United Kingdom*

The resolution limit in diffusion MRI determines the minimal structural size, e.g. axon diameter, that is possible to estimate accurately. In q-space analysis, this limit scales according to the inverse cube root of the maximal gradient strength ( $G_{max}$ ). In this study, we show by theoretical analysis and simulations that the resolution limit scales as the inverse square root of  $G_{max}$  for model-based diffusion MRI.

3568. 33 **Sub-Voxel Micro-Architecture Assessment**

**by Diffusion of Mechanical Shear Waves** 

Lauriane Jugé<sup>1</sup>, Simon Auguste Lambert<sup>1</sup>,  
Simon Chatelin<sup>1</sup>, Leon ter BEEK<sup>2</sup>, Valérie  
Vilgrain<sup>1</sup>, Bernard E Van BEERS<sup>1</sup>, Lynne E  
Bilston<sup>3</sup>, Bojan Guzina<sup>4</sup>, Sverre Holm<sup>5</sup>, and  
Ralph Sinkus<sup>1</sup>

<sup>1</sup>U773-CRB3, INSERM, Paris, France, <sup>2</sup>Philips  
Medical Systems, Best, Netherlands, <sup>3</sup>University  
of New South Wales, Neuroscience Research  
Australia, New South Wales, Australia, <sup>4</sup>Dept. of  
Civil Engineering, University of Minnesota,  
Minneapolis, MN, United States, <sup>5</sup>Informatics,  
University of Oslo, Oslo, Norway

In diffusion-weighted imaging, micro-structural information is lost due to the massive averaging that occurs within the imaging voxel and can only be revealed when exploring the tissue using different b-values. Similarly, for the first time we demonstrated using magnetic resonance elastography (MRE) that the frequency-dependence of mechanical shear wave diffusion can allow probing sub-voxel distributions of scattering structures and as a consequence overcome the spatial resolution limitation relying intrinsically on the MR imaging sensitivity. This technique opens perspective of detecting small metastases or neo-vascularisation which could really justify the use of MRE as a powerful clinical diagnosis tool.







3569.

34 **Measuring Cell Permeability with Diffusion-Weighted Simultaneous Spin-Echo and Stimulated Echo EPI**  

Sharon Peled<sup>1</sup>, Saadallah Ramadan<sup>2</sup>, and Carl-Fredrik Westin<sup>1</sup>

<sup>1</sup>Radiology, Brigham and Women's Hospital, Boston, MA, United States, <sup>2</sup>School of Health Sciences, University of Newcastle, Callaghan, NSW, Australia

A comparison of the spin echo and stimulated echo DWI signals may yield an in vivo biomarker reflecting the permeability and/or thickness of the myelin sheath. The spin echo and stimulated echo DW-EPI signals can both be measured after a single excitation.

3570. 35 **Measurement of post-mortem brain microstructure using a clinical MR scanner with oscillating gradients**    
 Wilfred W Lam<sup>1</sup>, Saad Jbabdi<sup>1</sup>, and Karla L Miller<sup>1</sup>  
<sup>1</sup>*FMRIB Centre, University of Oxford, Oxford, Oxon, United Kingdom*
- A model that fits the extracellular diffusivity spectrum of square-packed, non-abutting cylinders was developed and validated with simulation. A combination of sine- and cosine-modulated oscillating gradients provided sensitivity to the intracellular and extracellular compartments. Values for intracellular volume fraction, effective intracellular and extracellular radii, and diffusivity spectra of the splenium of a post-mortem macaque brain were acquired using a clinical MR scanner.
3571. 36 **Average Axon Diameter Mapping of Pig Spinal Cord Using d-PFG Filtered MRI**    
 Michal E Komlosh<sup>1,2</sup>, Evren Ozarslan<sup>1,3</sup>, Martin J Lizak<sup>4</sup>, Iren Horkayne-Szakaly<sup>5</sup>, Raisa Z Freidlin<sup>6</sup>, and Peter J Basser<sup>1</sup>  
<sup>1</sup>*STBB, PPITS, NICHD, NIH, Bethesda, MD, United States*, <sup>2</sup>*CNRM, USUHS, Bethesda, MD, United States*, <sup>3</sup>*CNRM, USUHS, United States*, <sup>4</sup>*NMRF, NINDS, NIH, Bethesda, MD, United States*, <sup>5</sup>*Neuropathology and Ophthalmic Pathology, Armed Forces Institute of Pathology, United States*, <sup>6</sup>*CIT, NIH, Bethesda, MD, United States*
- Double-PFG filtered MRI was used with a theoretical model to obtain an average fiber diameter map of fixed pig spinal cord. K-means segmentation and histological analysis were performed to verify the result. This study demonstrates that d-PFG filtered MRI is a powerful tool for mapping axon diameter, and potentially other microstructural features of tissues.
3572. 37 **The Rician bias in diffusion MRI: a technical overview**    
 Jelle Veraart<sup>1</sup>, and Jan Sijbers<sup>1</sup>  
<sup>1</sup>*Vision Lab, University of Antwerp, Antwerp, Belgium*

Many diffusion models require highly diffusion-weighted MR images, which suffer from low signal-to-noise ratio (SNR). Not only the precision of the diffusion model parameter estimators depends on the SNR, the estimator's accuracy will also be affected if the Rice distribution of magnitude MR data is not accounted for. We will give a technical overview of –on the one hand - the effect of the so-called Rician bias on diffusion model parameters - on the other hand – some techniques, which were proposed to reduce/remove the Rician bias.

3573.



38

### **Denoising Diffusion-Weighted MR Images Using Low Rank Structure and Edge Constraints**

**Constraints**  

Fan Lam<sup>1,2</sup>, S. Derin Babacan<sup>2</sup>, Norbert Schuff<sup>3</sup>, and Zhi-Pei Liang<sup>1,2</sup>



<sup>1</sup>*Electrical and Computer Engineering, University of Illinois at Urbana-Champaign, Urbana, IL, United States,* <sup>2</sup>*Beckman Institute, University of Illinois at Urbana-Champaign, Urbana, IL, United States,* <sup>3</sup>*Center for Imaging of Neurodegenerative Diseases, VA Medical Center, San Francisco, CA, United States*

A novel method is proposed to denoise diffusion weighted image sequences. The proposed method uses a penalized maximum likelihood formulation that handles Rician noise and incorporates low rank structure and prior edge information. The proposed method has been evaluated using experimental DTI data, and provides superior performance on recovering image features, anisotropy and orientation information of diffusion tensors originally corrupted by noise. We expect the proposed method to prove useful for achieving higher measurement precision and/or reducing data acquisition time for diffusion MRI.

3574.

39

### **Computed Diffusion Weighted Imaging under Rician Noise Distribution**

**under Rician Noise Distribution**  

Tokunori Kimura<sup>1</sup>, and Yuataka Machii<sup>1</sup>  
<sup>1</sup>*MRI development department, Toshiba Medical Systems Corp., Otawara, Tochigi, Japan*

A technique of computed diffusion weighted

imaging (cDWI) allowing to generate high b-value equivalent DWI images from low b-value images was assessed. In this study, simulation, phantom and volunteer study were performed to optimize b-values for the range of biologic tissue ADC under Rician noise. cDWI could provide better SNR images than the mDWI when original data SNRs were kept  $>3$ , by reducing background signals below noise bias which is problematic on standard mDWI. In conclusion, cDWI at optimum conditions can provide high CNR body diffusion imaging especially for higher ADC and shorter T2 tissues under Rician noise.

3575.

40

### **Conditional least squares estimation of diffusion MRI parameters**

Jelle Veraart<sup>1</sup>, Sofie Van Cauter<sup>2</sup>, Stefan Sunaert<sup>2</sup>, and Jan Sijbers<sup>1</sup>

<sup>1</sup>University of Antwerp, Antwerp, Antwerp, Belgium, <sup>2</sup>Department of Radiology, University Hospitals of Leuven, Leuven, Belgium

Many diffusion models require highly diffusion-weighted images, which suffer from low signal-to-noise ratio, eddy current distortions, and subject motion. Prior to diffusion model fitting, those distortions should be corrected; That data correction alters the underlying Rician data distribution. Therefore, previously proposed methods remove the Rician bias might be suboptimal. We propose a conditional least squares estimator (CLS), which is from theoretically an equivalent to the maximum likelihood estimator (MLE). However, the CLS remains, unlike the MLE, in well-defined cases unbiased after data correction as it can rely on the linearity of the expectation operator in high SNR and homogeneous regions.

3576.

41

### **The Parallel Kalman Filter: an efficient tool to deal with real-time non central $\chi$ noise correction**

Veronique Brion<sup>1</sup>, Olivier Riff<sup>1</sup>, Maxime Descoteaux<sup>2</sup>, Jean-François Mangin<sup>1</sup>, Denis Le Bihan<sup>1</sup>, Cyril Poupon<sup>1</sup>, and Fabrice Poupon<sup>1</sup>

<sup>1</sup>NeuroSpin, CEA/I<sup>2</sup>BM, Gif-sur-Yvette, France, <sup>2</sup>Sherbrooke University, Sherbrooke, Canada



This abstract proposes a novel real-time non central  $\chi$  noise correction method for diffusion-weighted MR data that are known to be particularly sensitive to noise, as the diffusion indicator in the tissues corresponds to a signal loss. The technique is based on a Parallel Kalman Filter which is well adapted for non-Gaussian noise distributions, and which is as suitable for real time purposes as the standard Kalman filter. The results on simulated and real HARDI data show that it outperforms the standard Kalman Filter approach since non-Gaussian noise distributions are directly embedded in the process through their Gaussian mixture approximation.

3577.

42

### **A Robust and Automated Method for Estimating the Expected Signal Standard Deviation in DWI Datasets**

Lin-Ching Chang<sup>1</sup>, and Carlo Pierpaoli<sup>2</sup>

<sup>1</sup>*Department of Electrical Engineering and Computer Science, The Catholic University of America, Washington, DC, United States,*

<sup>2</sup>*National Institutes of Health, Bethesda, MD, United States*

Correctly estimating the expected signal standard deviation (SD) due to thermal noise in diffusion weighted images (DWIs) is important for controlling image quality, correctly computing the chi-squares value, image registration and outlier detection. For single channel acquisitions, signal SD could be estimated from a ghost-free region of the image background. However, the signal in the background of DWIs acquired on modern clinical scanners cannot be used for this purpose. This paper proposes an object-based method taking advantage of robust regression and residual analysis to estimate signal SD. Results from simulation indicate that the proposed method performs very well even in the presence of DWI volumes which are completely corrupted.

3578.

43

### **Outlier Detection based on the Neural Network for Tensor Estimation**

Zhenyu Zhou<sup>1,2</sup>, Yijun Liu<sup>3</sup>, Guang Cao<sup>1</sup>, Karen M. von Deneen<sup>3</sup>, and Dongrong Xu<sup>2</sup>



<sup>1</sup>*Global Applied Science Laboratory, GE Healthcare, Beijing, Beijing, China,* <sup>2</sup>*MRI Unit,*

*Columbia University, New York, NY, United States, <sup>3</sup>McKnight Brain Institute, University of Florida, Gainesville, FL, United States*

Diffusion weighted imaging is always influenced by both thermal noise and spatially and/or temporally varying artifacts such as subject motion and cardiac pulsation. Motion artifacts are particularly prevalent, especially when scanning an uncooperative population with several disorders. In this study, we proposed a classifier work frame which can classify DWIs as normal images or motion artifacts. It achieves better performance in tensor estimation by automatic unvoxel-wise outlier rejection compared with manual and visual inspection, and previous voxel-wise outlier rejection methods. The proposed method could potentially remove the influence of unexpected motion artifacts in DWI acquisitions.

3579.

44

**Maximum likelihood ADC parameter estimates improve selection of metastatic cervical nodes for patients with head and neck squamous cell cancer**  

Nikolaos Dikaios<sup>1</sup>, Shonit Punwani<sup>2</sup>, Valentin Hamy<sup>1</sup>, Pierpaolo Purpura<sup>2</sup>, Heather Fitzke<sup>3</sup>, Scott Rice<sup>2</sup>, Stuart Taylor<sup>3</sup>, and David Atkinson<sup>3</sup>

<sup>1</sup>*Department of Medical Physics and Bioengineering, University College London, London, Greater London, United*

*Kingdom, <sup>2</sup>Department of Radiology, University College London Hospital, <sup>3</sup>Centre for Medical Imaging, University College London*

The aim of this work was to determine whether classification of benign and metastatic cervical nodes based on diffusion weighted imaging (DWI) could be improved by use of a maximum likelihood algorithm for derivation of ADC parameters. A non linear least squares (LSQ) algorithm is usually used to fit parameters to the measured MR signal intensities as a function of b-value. LSQ assumes that the noise in high b-values is normally distributed whereas in reality it follows a Rice distribution. To account for the Rician noise, maximum likelihood (ML) algorithms have been proposed that provide unbiased ADC estimates. In this work the monoexponential, stretched exponential and biexponential models were examined, with their involved parameters calculated using the LSQ

and the ML algorithms.

3580.

45

**DWI denoising using overcomplete Local PCA Decomposition**  

Jose V Manjon<sup>1</sup>, Pierrick Coupe<sup>2</sup>, Luis Concha<sup>3</sup>, Antoni Buades<sup>4</sup>, Louis Collins<sup>5</sup>, and Montserrat Robles<sup>6</sup>

<sup>1</sup>IBIME, UPV, valencia, Spain, <sup>2</sup>LaBRI, Bourdeaux, France, <sup>3</sup>UNAM, Mexico, <sup>4</sup>Universite Paris Descartes, France, <sup>5</sup>MNI, Canada, <sup>6</sup>IBIME, UPV, Valencia, Spain

Diffusion Weighted Images normally show a low SNR due to the presence of noise from the measurement process which complicates and potentially bias the estimation of the diffusion parameters. In this paper, a new denoising method is proposed which takes into consideration the multicomponent nature of DW images. This new filter reduces random noise in multicomponent Diffusion MR images by locally shrinking less significant Principal Components using an overcomplete approach. The proposed method is compared with similar state of art methods using synthetic and real clinical MR images showing an improved performance in all cases analyzed.

3581.



46

**Outlier detection for high b-value diffusion data**  



Kerstin Pannek<sup>1</sup>, David Raffelt<sup>2</sup>, Christopher Bell<sup>1</sup>, Jane Mathias<sup>3</sup>, and Stephen Rose<sup>1</sup>

<sup>1</sup>The University of Queensland, Brisbane, Queensland, Australia, <sup>2</sup>Brain Research Institute, Australia, <sup>3</sup>University of Adelaide, Australia

Diffusion weighted images are prone to artefacts caused by physiological noise. Existing model based approaches for voxel-wise identification of such artefacts rely on the diffusion tensor model, which is problematic in crossing fibre areas and at higher b-values required for high angular resolution diffusion imaging. We developed a voxel-wise identification method based on a higher order model of diffusion, and compared outlier probability maps obtained using the tensor model with those obtained using a higher order model in a cohort of 103 healthy participants.

3582. 47 **SNR-adaptive Inhomogeneous Noise Correction combined with Uniform filter and Sensitivity map (INCUS) applying to Diffusion Weighted Image with Parallel Imaging**    
Tokunori Kimura<sup>1</sup>, and Takashi Shigeta<sup>1</sup>  
<sup>1</sup>MRI development department, Toshiba Medical Systems Corp., Otawara, Tochigi, Japan

The purpose of this study was to assess a technique named INCUS (inhomogeneous noise correction combined with uniform filter and sensitivity map) for correcting spatially inhomogeneous noise on parallel imaging (PI) adaptively by combining with the Wiener filter (WF). Three types of WF were compared between INCUS and uniform type to DWI images. The INCUS could naturally reduce such noises while minimizing blur, and the minimum RMSE was smaller in the INCUS-WF than in the uniform-WF. We concluded that INCUS-WF is simple but very effective to optimally and automatically improve the spatially inhomogeneous noise on PI.

3583. 48 **Reliability of bi-exponential parameter estimation**    
Koichi Oshio<sup>1</sup>  
<sup>1</sup>Department of Diagnostic Radiology, Keio University School of Medicine, Shinjuku-ku, Tokyo, Japan

The shape of bi-exponential fitting errors in the parameter space was calculated and visualized. From these plots, it is suggested that parameter estimation with bi-exponential curve fitting is not reliable, even though the fitting itself is good, especially for small range of b-value. Using a new set of parameters, D and d, it is possible to estimate the parameters more reliably, and the parameter interpretation becomes more straightforward.

## Electronic Poster Session - Diffusion & Perfusion

---

## HARDI & Advanced Clinical DWI

Click on  to view the abstract pdf and click on  to view the video presentation. (Not all presentations are available.)

Tuesday 8 May 2012

Exhibition Hall

16:00 - 17:00

### Computer #

3584.



49

#### **HARDI-based methods for fiber orientation estimation**

Ben Jeurissen<sup>1</sup>, Alexander Leemans<sup>2</sup>, Jacques-Donald Tournier<sup>3,4</sup>, and Jan Sijbers<sup>1</sup>

<sup>1</sup>Vision Lab, University of Antwerp, Antwerp, Belgium, <sup>2</sup>Image Sciences Institute, University Medical Center Utrecht, Utrecht, Netherlands, <sup>3</sup>Brain Research Institute, Florey Neuroscience Institutes (Austin), Melbourne, Victoria, Australia, <sup>4</sup>Department of Medicine, University of Melbourne, Melbourne, Victoria, Australia

In voxels containing multiple fiber orientations, diffusion tensor imaging (DTI) has been shown to provide misleading white matter orientation 'integrity' information. Several methods have been proposed to extract fiber orientation information from the diffusion-weighted signal, many of them relying on the high angular resolution diffusion imaging (HARDI) protocol. The purpose of this presentation is to review the most widely-used methods for extracting fiber orientation information from single-shell HARDI data. From this overview, the need for multi-fiber reconstruction algorithms should be clear as well as the advantages and limitations of the different multi-fiber reconstruction methods.

3585.

50

#### **Assessing the implications of complex fiber configurations for DTI metrics in real data sets**

Ben Jeurissen<sup>1</sup>, Alexander Leemans<sup>2</sup>, Jacques-Donald Tournier<sup>3,4</sup>, Derek K Jones<sup>5</sup>, and Jan Sijbers<sup>1</sup>

<sup>1</sup>Vision Lab, University of Antwerp, Antwerp, Belgium, <sup>2</sup>Image Sciences Institute, University Medical Center Utrecht, Utrecht, Netherlands, <sup>3</sup>Brain Research Institute, Florey Neuroscience Institutes (Austin), Melbourne,

Victoria, Australia, <sup>4</sup>Department of Medicine, University of Melbourne, Melbourne, Victoria, Australia, <sup>5</sup>CUBRIC, School of Psychology, Cardiff University, Cardiff, United Kingdom

A recent study, using high quality diffusion weighted data and CSD, has shown that multiple fiber orientations can be detected consistently in approximately 90% of all WM voxels. In this work, we assess the impact on DTI fiber tractography and WM 'integrity' metrics by measuring: 1) the angle between the primary DTI eigenvector and the nearest CSD orientation; 2) the volume fraction of the non-dominant CSD fiber orientations. We show that errors in the DTI fiber orientations are widespread throughout the WM and that many voxels contain contributions from non-dominant orientations that would be sufficiently large to affect tensor-derived measures.

3586.

51 **Tract Coherence Imaging (TCI): Quantifying the intra-voxel fiber tract heterogeneity**  

Sjoerd B Vos<sup>1</sup>, Max A Viergever<sup>1</sup>, and Alexander Leemans<sup>1</sup>

<sup>1</sup>Image Sciences Institute, University Medical Center Utrecht, Utrecht, Netherlands

Complementary to track-density imaging (TDI), we have proposed tract coherence imaging, TCI, as a new MRI contrast to investigate the local architectural configuration of tract pathways. TCI quantifies the local consistency of fiber tract orientations for a given voxel resolution, limited between '0' (random orientations) and '1' (perfectly aligned fibers), providing an elegant framework for quantitative evaluations that can be used in a super-resolution framework. TCI does not depend on voxel size in homogenous tract configurations, facilitating quantitative analyses. Furthermore, the peak fiber orientations can be extracted from the tract pathways in each voxel to further understand the architectural complexity.

3587.

52 **An Optimization Protocol for Generalized Diffusion Tensor Imaging with Higher Order Tensors**  

Nicole Murphy<sup>1</sup>, Ching-Po Lin<sup>2</sup>, and Chunlei Liu<sup>3</sup>

<sup>1</sup>*Brain Imaging Analysis Center, Duke University, Durham, North Carolina, United States,* <sup>2</sup>*Department of Biomedical Imaging and Radiological Sciences, National Yang-Ming University, Taipei, N/A, Taiwan,* <sup>3</sup>*Department of Radiology, Duke University, Durham, NC\_3129, United States*

3588.

53

**Pitfalls in the Reconstruction of Fibre ODFs Using Spherical Deconvolution of Diffusion MRI Data**  

Greg D Parker<sup>1</sup>, and Derek K Jones<sup>1</sup>

<sup>1</sup>*CUBRIC, School of Psychology, Cardiff University, Cardiff, South Glamorgan, United Kingdom*

We report a previously overlooked pitfall in spherical deconvolution approaches for reconstructing fibre orientation distribution functions (fODFs) through a spherical-harmonic (SH) basis. By examining single-fibre population (fibres along the same axis) cases, we are able to uncover descriptive deficiencies in the SH representation that result in spurious fODF peaks once the assumed and actual diffusive properties of the target fibrous tissue no longer agree (e.g. local degradation through disease). Through comparison with an alternative that does not rely on spherical harmonics, we are also able to suggest a viable alternative for cases where a 'one-size-fits-all' single-fibre diffusivity assumption is inappropriate.

3589.

54

**Multi-directional anisotropy obtained from the diffusion propagator**  

Ek T Tan<sup>1</sup>, Luca Marinelli<sup>1</sup>, Christopher J Hardy<sup>1</sup>, Kevin F King<sup>2</sup>, Jonathan I Sperl<sup>3</sup>, and Marion I Menzel<sup>3</sup>

<sup>1</sup>*GE Global Research, Niskayuna, NY, United States,* <sup>2</sup>*GE Healthcare, Waukesha, WI, United States,* <sup>3</sup>*GE Global Research, Garching, Germany*

Diffusional anisotropy is an important indicator for axonal integrity, but conventional DTI-based fractional anisotropy (FA) is not well-suited to describing anisotropy of multi-directional diffusivities. A multi-directional anisotropy (MDA) metric was proposed, which is



analytically and experimentally shown to be equivalent to FA in single-fibers. In double-fibers, the mean MDA was higher than FA, while the variation of MDA was smaller than FA. In addition, fiber counts can be inferred from the diffusion propagator. The availability of both MDA and fiber counting can be useful for multi-parametric analysis of anisotropy in crossing-fiber and gray matter regions.

3590.

55

### **Fast DSI Acquisition and Reconstruction Based on Sparse Diffusion Propagator Representations**

Antonio Tristán-Vega<sup>1</sup>, and Carl-Fredrik Westin<sup>1</sup>

<sup>1</sup>*Laboratory of Mathematics in Imaging, Brigham and Women's Hospital, Boston, Massachusetts, United States*

Compressed Sensing grants the possibility of reducing the number of samples required to describe a signal below its Nyquist rate. When applied to the estimation of the diffusion propagator in diffusion spectrum imaging, it arises the need to find a basis for which the propagator is sparse, which is not trivial. We address this problem by two means: 1) mapping the propagator to a space where it is sparse, and 2) using a model that explicitly isolates a non-sparse residual. We provide two reconstruction algorithms for such model, notably improving the estimation accuracy and sparsity compared to previous approaches.

3591.

56

### **High angular resolution diffusion imaging methods: a diffusion phantom study**

Ezequiel Farrher<sup>1</sup>, Tony Stöcker<sup>1</sup>, Farida Grinberg<sup>1</sup>, and N. Jon Shah<sup>1,2</sup>

<sup>1</sup>*Institute of Neuroscience and Medicine - 4, Forschungszentrum Juelich, Juelich, Germany,* <sup>2</sup>*JARA - Faculty of Medicine, RWTH Aachen University, Aachen, Germany*

Diffusion-weighted magnetic resonance imaging provides a unique, non-invasive tool to characterize tissue microstructure and orientation. In order to enable a quantitative validation of the proposed physical models to elucidate tissue orientation, it is necessary to have artificial systems with well-known structure and physical properties. In this work,

we demonstrate the application of a multi-section diffusion phantom used for comparison of the performance of two models for high angular resolution diffusion imaging (HARDI) data analysis, i.e. the so-called Q-ball Imaging (QBI) and the constrained spherical deconvolution (CSD) methods.

3592.

57

**Quantification of fiber bundle properties using a decomposition of the fiber orientation distribution function**  

Till Riffert<sup>1</sup>, Thomas Knösche<sup>1</sup>, and Alfred Anwander<sup>1</sup>

<sup>1</sup>*Cortical Networks and Cognitive Functions, Max Planck Institute for Human Cognitive and Brain Sciences, Leipzig, Germany*

3593.

58

**Comparison of *In Vivo* Human, *In Vivo* Macaque and *Ex Vivo* Human Measurements of Diffusion Orientation in the Cerebral Cortex**  

Jennifer A. McNab<sup>1</sup>, Jonathan R Polimeni<sup>1</sup>, Ruopeng Wang<sup>1</sup>, Jean C. Augustinack<sup>1</sup>, Kyoko Fujimoto<sup>1</sup>, Allison Player<sup>1</sup>, Christina Triantafyllou<sup>1,2</sup>, Thomas Janssens<sup>3</sup>, Reza Farivar<sup>1</sup>, Wim Vanduffel<sup>1,3</sup>, and Lawrence L Wald<sup>1,4</sup>

<sup>1</sup>*A.A. Martinos Center for Biomedical Imaging, Radiology, Massachusetts General Hospital, Harvard Medical School, Boston, MA, United States*, <sup>2</sup>*A.A. Martinos Center at the McGovern Institute for Brain Research, Massachusetts Institute of Technology, Cambridge, MA, United States*, <sup>3</sup>*Laboratory for Neuro- and Psychophysiology, K.U. Leuven Medical School, Campus Gasthuisberg, Leuven, Belgium*, <sup>4</sup>*Harvard-MIT Health Sciences and Technology Division, Massachusetts Institute of Technology, Cambridge, MA, United States*

We compare cortical diffusion anisotropy in *in vivo* human (1 mm iso), *in vivo* macaque (0.7 mm iso) and in *ex vivo* human tissue (0.5 mm iso). All data sets show radial diffusion in M1 and tangential diffusion in S1, although the *ex vivo* human data also shows some regions of radial diffusion in S1.

3594.

59

### High-resolution diffusion-weighted imaging of the orientational structure of motor and somatosensory cortex in human cadaver brain

Christoph Wolfram Ulrich Leuze<sup>1</sup>, Alfred Anwander<sup>1</sup>, Stefan Geyer<sup>1</sup>, Pierre-Louis Bazin<sup>1</sup>, and Robert Turner<sup>1</sup>

<sup>1</sup>Max Planck Institute for Human Cognitive and Brain Sciences, Leipzig, Sachsen, Germany

Diffusion-weighted imaging (DWI) at high spatial and angular resolution was performed at 9.4 T on a block of fixed human cadaver brain tissue containing part of the motor-(M1) and somatosensory (S1) cortex. Analysis of the radially of the diffusion showed that, unlike stated in earlier studies, the prevalent diffusion direction in S1 is not entirely tangential but rather that neighbouring layers with alternating tangential and radial diffusion properties in both M1 and S1 exist. High DWI spatial resolution is therefore clearly of great importance for correct conclusions regarding cortical orientational structure in the cortex.

3595.

60

### Towards assessing spatial normalizations employing DTI and HARDI models

Luke Bloy<sup>1</sup>, Alex R Smith<sup>2</sup>, Madhura Ingalhalikar<sup>2</sup>, Robert T Schultz<sup>3</sup>, Timothy P.L. Roberts<sup>4</sup>, and Ragini Verma<sup>2</sup>

<sup>1</sup>Section of Biomedical Imaging, University of Pennsylvania, Philadelphia, PA, United States, <sup>2</sup>Section of Biomedical Imaging, Univeristy of Pennsylvania, Philadelphia, PA, United States, <sup>3</sup>Center for Autism Research, Children's Hospital of Philadelphia, Philadelphia, PA, United States, <sup>4</sup>Lurie Family Foundation's MEG Imaging Center, Children's Hospital of Philadelphia, Philadelphia, PA, United States

This study compares the results of using DTI and HARDI based diffusion models as the driving force behind spatial normalization algorithms. Each modality underwent separate state of the art registration pipelines designed to optimally take advantage of each contrast. The deformations resulting from each pipeline were applied to the images of the other modality, allowing for three means of comparison. Both registration pipelines perform

similarly when FA variance was used as a means of comparison, however using either FOD or normalized FOD variance HARDI registration performed better. This demonstrates the importance of using HARDI when accurate registration is required.

3596.

61

### **Diffusion-weighted Spectroscopic Imaging of Multiple Metabolites in Rat Brains after Middle Cerebral Artery Occlusion**

Yoshitaka Bito<sup>1</sup>, Yuko Kawai<sup>2</sup>, Koji Hirata<sup>1</sup>, Toshihiko Ebisu<sup>3</sup>, Yosuke Otake<sup>1</sup>, Satoshi Hirata<sup>1</sup>, Toru Shirai<sup>1</sup>, Yoshihisa Soutome<sup>1</sup>, Hisaaki Ochi<sup>1</sup>, Masahiro Umeda<sup>2</sup>, Toshihiro Higuchi<sup>4</sup>, and Chuzo Tanaka<sup>4</sup>

<sup>1</sup>Central Research Laboratory, Hitachi, Ltd., Kokubunji-shi, Tokyo, Japan, <sup>2</sup>Medical Informatics, Meiji University of Integrative Medicine, Kyoto, Japan, <sup>3</sup>Neurosurgery, Nantan General Hospital, Kyoto, Japan, <sup>4</sup>Neurosurgery, Meiji University of Integrative Medicine, Kyoto, Japan

Diffusion-weighted echo-planar spectroscopic imaging with a pair of bipolar diffusion gradients (DW-EPSI with BPGs) was used to acquire changes in apparent diffusion coefficient (ADC) for multiple metabolites, namely, N-acetylaspartate (NAA), creatine (Cr) and choline (Cho), in rat brains after a right middle cerebral artery occlusion (MCAO). The acquired changes in ADC maps of the metabolites and water were analyzed by using Gaussian mixture distribution, which takes advantage of the multiple spatial pixels acquired simultaneously by diffusion-weighted spectroscopic imaging. It is shown that DW-EPSI with BPGs is effective for investigating spatially varying ADC changes for metabolites and that this technique may be useful for understanding intra-cellular dynamics by using multiple metabolites as probes.

3597.

62

### **Assessing Anti-inflammation and Axonal Preservation Effect of FTY720 Using Diffusion MRI**

Xiaojie Wang<sup>1</sup>, Yong Wang<sup>2</sup>, Cheryl Nutter<sup>3</sup>, and Sheng-Kwei Song<sup>2</sup>

<sup>1</sup>Chemistry, Washington University, Saint Louis, Missouri, United States, <sup>2</sup>Radiology, Washington University, Saint Louis, United States, <sup>3</sup>Pfizer



*Inc., United States*

Multiple sclerosis (MS) is an inflammatory demyelinating disease with axonal injury causing permanent neurological disabilities. Axonal preservation remains a significant challenge in current anti-inflammatory therapies of MS. In the present study, we demonstrate the efficacy of anti-inflammation and axonal preservation of FTY720 on experimental autoimmune encephalomyelitis (EAE) mice examined using diffusion MRI. The effect of increased cellularity and vasogenic edema associated with inflammation on diffusion tensor imaging parameters was also examined.

3598.



63

**Diffusion Basis Spectrum Imaging detects evolving axonal injury, demyelination and inflammation in the course of EAE**  



Tsang-Wei Tu<sup>1</sup>, Yong Wang<sup>2</sup>, Chia-Wen Chiang<sup>3</sup>, Tsen-Hsuen Lin<sup>4</sup>, Ying-Jr Chen<sup>3</sup>, Anne Cross<sup>5</sup>, and Sheng-Kwei Song<sup>2</sup>

<sup>1</sup>Radiology, Washington University, Saint Louis, Missouri, United States, <sup>2</sup>Radiology, Washington University, <sup>3</sup>Chemistry, Washington University, <sup>4</sup>Physics, Washington University, <sup>5</sup>Neurology, Washington University

A novel diffusion basis spectrum imaging (DBSI) was recently introduced to resolve inflammation in presence of axon and myelin damage in a mouse model of multiple sclerosis. Besides the anisotropic indices provided by DTI, the isotropic diffusion reflects inflammation, through the estimation of cellularity and water fraction. In current study, in vivo DBSI of the lumbar spinal cord from EAE mice was performed, followed by histological validation. DBSI parameters revealed evolving multiple neuropathologies in the EAE course. Histological findings substantiated in vivo DBSI results. The quantification of cell and water fractions successfully identified the spatial and temporal evolution of inflammation.

3599.

64

**Increase of structural disorder along neurites is leading cause for diffusivity drop in acute ischemia**  

Dmitry S. Novikov<sup>1</sup>, Jens H. Jensen<sup>2</sup>, and

Joseph A. Helpern<sup>2</sup>

<sup>1</sup>Radiology, NYU School of Medicine, New York, NY, United States, <sup>2</sup>Radiology and Radiological Science, Medical University of South Carolina, Charleston, SC, United States

The types of microstructural architecture in any media (including living tissues) are classified in terms of the long-time tail exponent in the molecular velocity autocorrelation function. The specific value of the power-law exponent obtained from the oscillating gradient spin echo measurement in rat cerebral gray matter characterizes the relevant tissue anatomy that restricts water diffusion. It is argued that short-range disorder, likely due to spines and varicosities, provides the chief hindrance to diffusion along dendrites and axons and that the increase in this structural disorder is a primary cause of the diffusivity drop in ischemic stroke.

3600.



65

**Direct evidence for decreased intra-axonal diffusivity in ischemic human stroke**  

Els Fieremans<sup>1</sup>, Jens H. Jensen<sup>2</sup>, Edward S. Hui<sup>2</sup>, Dmitry S. Novikov<sup>1</sup>, Ali Tabesh<sup>2</sup>, Leonardo Bonilha<sup>2</sup>, and Joseph A. Helpern<sup>2</sup>

<sup>1</sup>Center for Biomedical Imaging, Radiology, New York University School of Medicine, New York, NY, United States, <sup>2</sup>Radiology and Radiological Science, Medical University of South Carolina, Charleston, SC, United States

The decrease of the water diffusion coefficient in ischemic stroke provides a sensitive and reliable diagnostic tool. However, the underlying biophysical mechanisms for the diffusion drop are still not fully understood. In this study, we characterize changes in the white matter microstructure in human subacute stroke by applying a recently developed white matter model for diffusional kurtosis imaging, which yields estimates for the intra-axonal and extra-axonal diffusivities and for the axonal water fraction. A large change of 55% is observed in the intra-axonal diffusivity, consistent with axonal beading as a primary mechanism underlying the diffusion drop associated with ischemia.

3601.

66

**Diffusional Kurtosis Imaging Detects Age-**

### related Grey matter Changes in the Normal Mouse Brain

Maria F Falangola<sup>1</sup>, David Guilfoyle<sup>2</sup>, Edward S Hui<sup>1</sup>, Caixia Hu<sup>2</sup>, Scott Gerum<sup>2</sup>, John LaFrancois<sup>3</sup>, Xingju Nie<sup>1</sup>, Jens Jensen<sup>1</sup>, Ali Tabesh<sup>1</sup>, and Joseph A Helpert<sup>1</sup>

<sup>1</sup>Radiology, Medical University of South Carolina (MUSC), Charleston, SC, United States,

<sup>2</sup>Medical Physics, Nathan Kline Institute, Orangeburg, New York, NY, United States,

<sup>3</sup>Dementia Research, Nathan Kline Institute, Orangeburg, New York, NY, United States

Since the transition from young to aged adult during the normal aging process leads to changes in grey matter morphology, characterizing the age-related diffusion patterns in the rodent brain is important for interpreting and differentiating the changes associated with pathological process in rodents' models of neurodegenerative diseases. Diffusional Kurtosis Imaging (DKI) quantifies the non-Gaussian behavior of water diffusion, contributing additional information beyond that provided by diffusion tensor imaging. Here we report that the DKI can characterize the age-related microstructural changes in the cortex and sub-cortical regions in the normal mouse brain.

3602.

### 67 High resolution ex vivo diffusion kurtosis imaging of chronic perilesional brain changes in a rat stroke model

Umesh Rudrapatna<sup>1</sup>, Pavel Yanev<sup>1</sup>, Karsten Ruscher<sup>2</sup>, Annette van der Toorn<sup>1</sup>, Tadeusz Wieloch<sup>2</sup>, and Rick Dijkhuizen<sup>1</sup>

<sup>1</sup>Biomedical MR Imaging and Spectroscopy Group, Image Sciences Institute, University Medical Center Utrecht, Utrecht,

Netherlands, <sup>2</sup>Laboratory for Experimental Brain Research, Department of Clinical Sciences Lund, Lund University, Lund, Sweden

Elucidation of structural plasticity in lesion borderzones after stroke may lead to development of recovery-enhancing strategies. While diffusion tensor imaging (DTI) allows assessment of white matter reorganization, there is no established MR contrast for measurement of structural remodeling in grey matter. In this study we analyzed to what



degree diffusion kurtosis imaging (DKI) allows detection of microstructural changes in perilesional grey matter. Our high resolution *ex vivo* study in a rat stroke model shows that at chronic time points, DKI parameters were significantly altered in perilesional cortex and striatum, and to a larger extent than DTI parameters. We speculate that DKI may significantly help to unravel the complex, heterogeneous microstructural changes associated with post-stroke tissue plasticity.

3603.

68

**Diffusion Kurtosis Imaging Analysis of Microstructural Differences between Patients with Alzheimer's Disease and Mild Cognitive Impairment**  

Nanjie Gong<sup>1</sup>, Chun Sing Wong<sup>1</sup>, Chun Chung Chan<sup>2</sup>, Lam Ming Leung<sup>2</sup>, Yiu Ching Chu<sup>3</sup>, and Queenie Chan<sup>4</sup>

<sup>1</sup>*Diagnostic Radiology, The University of Hong Kong, Hong Kong, China,* <sup>2</sup>*United Christian Hospital, Hong Kong,* <sup>3</sup>*Kwong Wah Hospital, Hong Kong,* <sup>4</sup>*Philips Healthcare, Hong Kong*

To investigate the sensitivity of the measurements from DKI for differentiating between patients with MCI and patients with AD and detecting microstructural changes in both white matter and grey matter, we used region of interest (ROI) analysis focusing on the ROIs that have been previously investigated using DTI model in other studies. We hypothesize that with more precise model and additional information provided by DKI matrix, we could not only better differentiate between MCI and AD, but also better characterize the microstructural alternations. This study was approved by Institutional Review Board in Hong Kong. From 2011/03-2011/09, totally 24 patients (13 male, 11 female) were recruited from a local tertiary referring center. While none previous studies, in which DTI model were used, of Alzheimer's disease and MCI found any significant difference between these two groups in regions like whole brain grey matter, temporal lobe white matter or grey matter, our study, with a more precise diffusion model of DKI, found promising difference in these regions which may characterize brain tissue microstructural changes during the disease deteriorating. In addition, the extra measurement of Kaxial bears possibility of providing information in new aspects which will

help improve the understanding and delineation of this disease. Further, only a few studies had demonstrated the correlation between MD or FA and MMSE score, and the results were controversial. It is worth noting that in our study, in addition to MD and FA, Daxial and Dradial along with the new measurements of Kaxial, Kradial, and MK also significantly correlated with MMSE score. It suggests that DKI models measurements may be more sensitive indicators for reflecting Alzheimer's disease progression.

3604.

69

### **Diffusional kurtosis imaging: Towards optimal subacute assessment of the microenvironment of ischemic tissue**

Edward S. Hui<sup>1</sup>, Chu-Yu Lee<sup>2</sup>, Josef P. Debbins<sup>2</sup>, Timothy Q. Duong<sup>3</sup>, and Joseph A. Helpert<sup>1</sup>

<sup>1</sup>Dept of Radiology, Medical University of South Carolina, Charleston, South Carolina, United States, <sup>2</sup>Dept of Electrical Engineering, Arizona State University, Tempe, Arizona, United States, <sup>3</sup>Research Imaging Institute, UTHSCSA, San Antonio, Texas, United States

The diagnostic value of ADC obtained from DWI is often dwarfed by its pseudonormalization during subacute stroke. It is therefore necessary to find an alternative that is more sensitive and specific to the underlying structural changes along the course of ischemic infarction. One potential technique is diffusion kurtosis imaging (DKI) which measures non-Gaussianity of water diffusion. The current study showed that MK is a sensitive biomarker for ischemic injury, especially subacute stroke where MD and T2W pseudonormalize as a result of vasogenic edema. DKI could potentially complement conventional DWI for improving stroke diagnosis, particularly during the subacute phase.

3605.

70

### **Diffusion Tensor and Kurtosis Imaging Analysis of Idiopathic Normal Pressure Hydrocephalus: by Using Corticospinal Tract**

Issei Fukunaga<sup>1,2</sup>, Masaaki Hori<sup>2</sup>, Yoshitaka Masutani<sup>3</sup>, Nozomi Hamasaki<sup>2</sup>, Shuuji Sato<sup>2</sup>, Takaaki Hattori<sup>4</sup>, Koji Kamagata<sup>2</sup>, Masakazu Miyajima<sup>5</sup>, Madoka Nakajima<sup>5</sup>, Atsushi

Nakanishi<sup>2</sup>, Shigeki Aoki<sup>2</sup>, and Atsushi Senoo<sup>1</sup>  
<sup>1</sup>Graduate School of Health Promotion Science, Tokyo Metropolitan University, Nerima ward, Tokyo, Japan, <sup>2</sup>Department of Radiology, Juntendo University, Bunkyo ward, Tokyo, Japan, <sup>3</sup>Department of Radiology, Graduate School of Medicine, The University of Tokyo, Bunkyo ward, Tokyo, Japan, <sup>4</sup>Department of Neurology, Kanto Central Hospital, Setagawa ward, Tokyo, Japan, <sup>5</sup>Department of Neurosurgery, Juntendo University, Bunkyo ward, Tokyo, Japan

We studied the diffusion characteristics of the brain in patients with idiopathic normal pressure hydrocephalus and in age-matched controls by using tract-specific analysis.

3606.

71 **Water Diffusional Kurtosis Imaging (DKI) Analysis of Ischemic Stroke Model in Juvenile Rats**  

Renaud NICOLAS<sup>1</sup>, Gérard RAFFARD<sup>2</sup>, Stéphane SANCHEZ<sup>2</sup>, Eric PETERSON<sup>2</sup>, Florent AUBRY<sup>1</sup>, Isabelle BERRY<sup>1</sup>, Pierre CELSIS<sup>1</sup>, and Bassem HIBA<sup>2</sup>

<sup>1</sup>Imagerie cérébrale et handicaps neurologiques; UMR 825, INSERM, F-31059 Toulouse, France, <sup>2</sup>Centre de Résonance Magnétique des Systèmes Biologiques, UMR 5536, CNRS, F-33076 Bordeaux, France

DWI images of 7 juvenile rats following MCAO were acquired with b-factors up to 2500 s/mm<sup>2</sup> and with three diffusion times (10,30,50 ms) and analysed with the Statistical Model of Diffusion Imaging that provide a way to estimate Diffusional Kurtosis of ischemic brain regions. A statistically significant change for Dapp (40 % reduction) and Kapp (55 % rise) were observed in ischemic versus healthy cortex. No significant effects of diffusion times were observed in this preliminary study.

3607.



72 **Diffusivity/Kurtosis Mismatch in Acute Ischemic Stroke: Potential Indicator of Reversible Ischemic Injury**  

Jerry S Cheung<sup>1</sup>, Enfeng Wang<sup>1,2</sup>, and Phillip Zhe Sun<sup>1</sup>

<sup>1</sup>Athinoula A. Martinos Center for Biomedical



*Imaging, Department of Radiology, MGH and Harvard Medical School, Charleston, MA 02129, United States, <sup>2</sup>Department of Radiology, 3rd Affiliated Hospital, Zhengzhou University, China*

By providing detailed properties on water diffusion and therefore more specific information on microstructural environment, diffusional kurtosis imaging (DKI) may allow better characterization on heterogeneous ischemic cerebral tissue. In this study, we examined and compared mean diffusion (MD) and mean kurtosis (MK) lesions in a transient middle cerebral artery occlusion (MCAO) ischemia rat model. Our results demonstrated that substantial mismatch between MD and MK lesions existed during MCAO, yet largely vanished following reperfusion. These initial findings suggest that diffusional kurtosis in addition to water diffusivity may improve understanding of the diffusion changes related to microstructural disturbances following acute cerebral ischemic injury.

## Electronic Poster Session - Diffusion & Perfusion

---

### Connectivity, Networks, & Kurtosis

Click on  to view the abstract pdf and click on  to view the video presentation. (Not all presentations are available.)

Tuesday 8 May 2012





Exhibition Hall

17:00 - 18:00

---

#### Computer

#

- |       |    |  |
|-------|----|--|
| 3608. | 49 | <p><b>Exploring the Structure of the Thalamus with DTI</b>  </p> <p>Sarah Mang<sup>1</sup></p> <p><sup>1</sup>German Cancer Research Center DKFZ, Heidelberg, DE, Germany</p> <p>Presentation and comparison of different DTI based methods for the segmentation of substructures in the Thalamus. Advantages and disadvantages of the different method types are discussed.</p> |
| 3609. | 50 | <p><b>Quantitative Analysis of Structural Connectivity Using Fiber Tracking and Non-Parametric Statistics</b>  </p>  |

Bagrat Amirbekian<sup>1,2</sup>, and Roland Henry<sup>1</sup>

<sup>1</sup>University of California San Francisco, San Francisco, California, United States, <sup>2</sup>UC Berkeley & UCSF Graduate Program in Bioengineering, San Francisco, California, United States

Fiber tracking is a powerful method to explore structural connectivity of white matter. However, without statistical methods to estimate the uncertainties associated with quantitative connectivity measures it is very hard to compare fiber tracking results. This study looks at the possibility of using the residual bootstrap with fiber tracking to establish confidence intervals on connectivity measures.

3610. 51 **Validation of DTI-tractography-based measures of white matter pathways originating from the primary motor area**  

Yurui Gao<sup>1,2</sup>, Ann S. Choe<sup>1,2</sup>, Xia Li<sup>1</sup>, Iwona Stepniewska<sup>3</sup>, and Adam W. Anderson<sup>1,4</sup>

<sup>1</sup>VUIIS, Vanderbilt University, Nashville, TN, United States, <sup>2</sup>BME, Vanderbilt University, Nashville, TN, United States, <sup>3</sup>Psychology, Vanderbilt University, Nashville, TN, United States, <sup>4</sup>BME, Radiology and Radiological Science, Vanderbilt University, Nashville, TN, United States

In our previous study, we validated DTI-tractography-based measures of primary motor area (M1) cortical-cortical connectivity. To further understand our previous result of validation, in this study we investigated the agreement between DTI-tractography-derived white matter pathways and histological pathways. We reconstructed the 3D pathway of histological fibers as well as DTI fibers originating from the M1 forelimb subarea in the squirrel monkey and then quantitatively measured the agreement between the DTI-derived pathway and the histology. We also describe potential reasons for the failure of DTI tractography to align perfectly with histological tracts.

3611. 52 **A semi-automatic approach for the extraction of white matter fiber bundles across subjects**  

Christian Ros<sup>1</sup>, Daniel Güllmar<sup>1</sup>, Martin Stenzel<sup>2</sup>, Hans-Joachim Mentzel<sup>2</sup>, and Jürgen Rainer Reichenbach<sup>1</sup>

<sup>1</sup>Medical Physics Group, Department for Diagnostic and Interventional Radiology I, Jena University Hospital, Jena, Thuringia, Germany, <sup>2</sup>Pediatric Radiology, Department for Diagnostic and Interventional Radiology I, Jena University Hospital, Jena, Thuringia, Germany

With this contribution we present a new method for the semi-automatic, consistent extraction of fiber bundles from multiple tractography data sets. For every fiber bundle, reliability maps were computed to assess the contribution of every voxel to the bundle. The reliability maps were then used to classify the fiber tracts of each data set. Due to the use of multiple tractography data sets, we were able to correct erroneous or wrongly labeled tracts that usually occur in individual data sets. Resulting fiber bundles are more consistent across subjects compared to bundles that are extracted with the ROI based methods.

3612. 53 **Comparison of thalamus parcellation by cortical projections using three tractography methods in neonates**  

Angela Downing<sup>1</sup>, Serena J Counsell<sup>1</sup>, Daniel Rueckert<sup>2</sup>, A David Edwards<sup>1</sup>, and Jo V Hajnal<sup>1</sup>

<sup>1</sup>Robert Steiner MRI Unit, Imaging Sciences Department, MRC Clinical Sciences Centre, Hammersmith Hospital, Imperial College, London, London, United Kingdom, <sup>2</sup>Department of Computing, Imperial College, London, London, United Kingdom

The development of thalamo-cortical projections is a key process in neonatal brain development. Parcellation of the thalamus according to thalamo-cortical connections found from DTI is becoming well established in adults but is currently uncertain in neonates. We have tested three methods, partial volume, constrained spherical deconvolution and global fibre reconstruction, using 32-direction HARDI data in term infants. Each method provided a parcellation in all cases and these were consistent to >63%. Whole brain seeding approaches were found to be the most consistent with each other and across subjects, as opposed to just considering paths seeded in the thalamus.







3613. 54 **Hippocampal subfield ICA multifiber tractography using 3T clinical diffusion data**  

Manbir Singh<sup>1</sup>, and Bryce Wilkins<sup>1</sup>

<sup>1</sup>Radiology and Biomedical Engineering, University of Southern California, Los Angeles, CA, United States

Hippocampal connectivity is a key objective of many clinical studies particularly of elderly subjects. Using a recently reported multi-fiber per voxel streamline tractography approach that can construct up to 3 fiber orientations per voxel in DTI data acquired with as few as 25 gradient directions, and hippocampal subfield demarcation by FreeSurfer, we show tracts connecting individual hippocampal subfields to the entire brain. Despite partial volume effects of the 2x2x2 mm<sup>3</sup> DTI acquisition, which would lead to overlapping tracts, differences in the subfield connections consistent with biologically known


hippocampal connectivity are apparent in these results.

3614. 55 **Visualizing tractography metrics of cortical-connectivity integrity in diffusion imaging**    
 Radu Jianu<sup>1</sup>, Wenjin Zhou<sup>1</sup>, Ryan Cabeen<sup>1</sup>, Daniel Dickstein<sup>2,3</sup>, and David H. Laidlaw<sup>1</sup>  
*<sup>1</sup>Computer Science, Brown University, Providence, RI, United States, <sup>2</sup>Psychiatry & Human Behavior, Brown University, Providence, RI, United States, <sup>3</sup>Bradley Hospital, Providence, RI, United States*
- We present a circular visualization interface of the tractography metrics for assessing cortical-connectivity integrity. We subdivided the gray matter into 80 regions-of-interest (ROIs) and calculated two metrics for each region-pair from the whole-brain tractography model produced from high angular resolution diffusion imaging. Three healthy control (HC) and three bipolar patients (BP) were examined in the visualization for their difference and location-specific changes in tractography metrics were identified.
3615. 56 **Variance of structural network for different fiber tracking schemes**    
 Hu Cheng<sup>1</sup>, Ruopeng Wang<sup>2</sup>, and Aina Puce<sup>1</sup>  
*<sup>1</sup>Indiana University, Bloomington, IN, United States, <sup>2</sup>Harvard University, Boston, MA, United States*
- We investigated the effect of different fiber tracking schemes on the construction of structural brain networks. Our results show that HARDI and DTI, FACT and Tensorline, both result in similar networks with correlation coefficients greater than 0.9. HARDI is superior to DTI in terms of tracking efficiency and test-retest reliability. Tensorline algorithm is able to track longer fibers than FACT but also produces more variances. The use of white matter mask can effectively remove spurious fibers that normally cannot survive over long range tracking. The networks constructed with and without white matter mask are very different.
3616. 57 **Neocortical Network Damage Assessment by Homotopic Lesion Mapping on Healthy Subjects**    
 Emil Harald Jeroen Nijhuis<sup>1,2</sup>, Douwe P Bergsma<sup>3,4</sup>, Albert V van den Berg<sup>5,6</sup>, Anne-Marie van Cappellen van Walsum<sup>2,7</sup>, and David G Norris<sup>1,8</sup>  
*<sup>1</sup>Donders Institute for Brain, Cognition and Behaviour, Radboud University, Nijmegen, Gelderland, Netherlands, <sup>2</sup>MIRA Institute for Biomedical Technology and Technical Medicine, University of Twente, Enschede, Overijssel, Netherlands, <sup>3</sup>Department of*



*Functional Neurobiology, Utrecht University, Helmholtz Research School, Netherlands, <sup>4</sup>Department of Cognitive Neuroscience, University Medical Centre St Radboud, Netherlands, <sup>5</sup>Department of Cognitive Neuroscience, Utrecht University, Helmholtz Research School, Netherlands, <sup>6</sup>Department of Cognitive Neuroscience, University Medical Centre St Radboud, Nijmegen, Netherlands, <sup>7</sup>Department of Anatomy, University Medical Centre St Radboud, Nijmegen, Netherlands, <sup>8</sup>Erwin L Hahn Institute for MRI, Universität Duisburg-Essen, Germany*

To determine the impact of a cerebral lesion on the neocortical network it is necessary to know its state in unharmed condition. We circumvent this problem by homotopically mapping a lesion to a healthy sample population and simulating its impact using a reachability and distance based measure.

3617. 58 **Whole-brain patterns of structural connectivity predict neurodevelopmental outcome in premature infants**  

Anand Pandit<sup>1</sup>, Emma Robinson<sup>2</sup>, Paul Aljabar<sup>3</sup>, Ioannis S Gousias<sup>1</sup>, Daniel Rueckert<sup>3</sup>, Serena J Counsell<sup>1</sup>, and David Edwards<sup>1</sup>

<sup>1</sup>Centre for the Developing Brain, MRC/Imperial College, London, London, United Kingdom, <sup>2</sup>FMRIB, University of Oxford, Oxford, United Kingdom, <sup>3</sup>Department of Computing, Imperial College, London, London, United Kingdom

In this study we combine a novel probabilistic tractography framework with Elastic Net LASSO regression in order to identify the structural connectivity patterns which are most predictive of neurodevelopmental outcome in prematurely born two-year old infants. Specific connections are shown to be responsible for effective neurological function. This work represents the first combined application of the tractography framework and regression method to this type of imaging data.

3618. 59 **Evaluating Tractography in Spatially Normalized DTI Data**  

Nagesh Adluru<sup>1</sup>, Do P. M. Tromp<sup>1</sup>, Hui Zhang<sup>2</sup>, and Andrew L. Alexander<sup>1</sup>


<sup>1</sup>University of Wisconsin-Madison, Madison, WI, United States, <sup>2</sup>University College London, United Kingdom

Tract specific analyses allow for statistical mapping of individual differences in specific white matter (WM) pathways. A crucial step involved in such advanced analyses is performing tractography in spatially normalized diffusion tensor imaging



(DTI) data. Spatial normalization of DTI data often involves highly non-linear transformations of the acquired data with embedded interpolations of the data. Our study aims at investigating the effects of such transformations on the anatomical consistency of the normalized space tractography compared to the acquired space tractography. Our results demonstrate that DTI spatial normalization does preserve properties of WM tractography with a high degree of consistency.

3619. 60 **Inter hemispheric transfer time and axon diameter properties of the corpus callosum**    
 Assaf Horowitz<sup>1</sup>, Daniel Barazany<sup>2</sup>, Galit Yovel<sup>2</sup>, and Yaniv Assaf<sup>2</sup>  
<sup>1</sup>Tel Aviv University, Tel Aviv, Israel, <sup>2</sup>Tel Aviv University



The corpus callosum (CC) is one of the largest fiber systems in the brain connecting and transferring information between the two hemispheres. Axcaliber is a diffusion MRI methodology the thorough analysis of multi-diffusion time, high b value DWI acquisition, allows the estimation of the axon diameter distribution (ADD). In this study we aimed to examine the inter-hemispheric transfer time (IHTT) and its relation to different axonal properties of the CC. We found that the ADD micro-structural differences at different parts of the CC are the base for the behavioral reaction time (IHTT) differences.

3620. 61 **Resolving Non-Gaussian Diffusion in Mouse Trigeminal Nerve using both Diffusion Kurtosis Imaging (DKI) and Diffusion Basis Spectrum Imaging (DBSI)**    
 Yong Wang<sup>1</sup>, Els Fieremans<sup>2</sup>, Peng Sun<sup>1</sup>, and Sheng-Kwei Song<sup>1</sup>  
<sup>1</sup>Radiology, Washington University in St. Louis, Saint Louis, MO, United States, <sup>2</sup>Radiology, New York University, New York, NY, United States



Diffusion kurtosis imaging (DKI) has been proposed as a clinically feasible method to estimate the intra- and extra-axonal diffusivities, and the intra-axonal water fraction. Diffusion basis spectrum imaging (DBSI) has been recently introduced to model multiple diffusion compartments of crossing fibers and inflammatory response in white matter injury. We hypothesize that by incorporating restricted intra-axonal water diffusion component, DBSI can also quantify the intra-axonal water fraction. In this study, DBSI and DKI are applied to mouse trigeminal nerves. Preliminary results have demonstrated that DBSI obtained similar estimation on both intra-axonal water fraction and other associated indices as DKI counterparts.

3621. 62 **Analysis of Effect of Short Diffusion Time in Diffusion Kurtosis Imaging using Oscillating Gradient**    
 Matthew M. Cheung<sup>1,2</sup>, Leon C. Ho<sup>1,2</sup>, Abby Y. Ding<sup>1,2</sup>, Condon Lau<sup>1,2</sup>, and Ed X. Wu<sup>1,2</sup>  
<sup>1</sup>Biomedical Imaging and Signal Processing, The University of Hong Kong, Pokfulam, Hong Kong SAR, China, <sup>2</sup>Department of Electrical and Electronic Engineering, The University of Hong Kong, Pokfulam, Hong Kong SAR, China

It has been known that kurtosis measurements are dependent on the diffusion time ( $\Delta$ ), due to restricted diffusion, heterogeneity of diffusion compartments or water exchange over different compartments. In this study, we applied oscillating diffusion gradient to investigate the diffusion time effect to DKI measurements in rat brain tissues in vivo. Mean diffusivity and kurtosis were found to increase and decrease respectively with  $\Delta$ , indicating increased restriction and microstructure heterogeneity. The  $\Delta$  dependency may provide insights into the complex cellular properties in normal and diseased neural tissues.

3622. 63 **General closed-form expressions for DKI parameters and their application to fast and robust DKI computation based on outlier removal**    
 Yoshitaka Masutani<sup>1</sup>, and Shigeki Aoki<sup>2</sup>  
<sup>1</sup>Radiology, The University of Tokyo Hospital, Bunkyo-ku, Tokyo, Japan, <sup>2</sup>Radiology, Juntendo Hospital, Bunkyo-ku, Tokyo, Japan

Non-Gaussianity quantification of water diffusion through diffusional kurtosis imaging (DKI) is expected in clinical applications such as classification of abnormal tissues. For faster computation of DKI parameters;  $K$ ,  $D$ , and  $S_0$ , we show that it is possible to obtain general closed-form expressions also for data sets by more than three  $b$ -values. In addition, we propose a fast and robust computation technique based on greedy removal of outlier sample pair of  $b$ -value and DWI signal. By using six data sets of brain from clinical MR scanner, the technique was proved to be fast, robust and effective for clinical DKI.

3623. 64 **Local variations of magnetic susceptibility affect the contrast of Kurtosis maps: validation in phantom at 9.4T and in human brain at 3T.**    
 Marco Palombo<sup>1,2</sup>, Silvia Gentili<sup>1</sup>, Silvia De Santis<sup>1,3</sup>, Marco Bozzali<sup>4</sup>, and Silvia Capuani<sup>1,2</sup>

<sup>1</sup>"Sapienza" University of Rome, Physics Department, Rome, Rome, Italy, <sup>2</sup>CNR-IPCF UOS Roma, "Sapienza" University of Rome, Rome, Rome, Italy, <sup>3</sup>CUBRIC, School of Psychology, Cardiff University, Cardiff, United Kingdom, <sup>4</sup>ISC - CNR Rome, Neuroimaging Laboratory Santa Lucia Foundation, Rome, Rome, Italy

The goal of this work was to investigate the influence of magnetic susceptibility ( $\Delta\chi$ ) variations (quantified by the T2\* parameter) on non-Gaussian water diffusion, evaluated by means of Diffusional Kurtosis Imaging method. To make our investigation more significant, the dependence of kurtosis indices were studied in both controlled phantom (characterized by pore size from 4 to 10  $\mu\text{m}$  and  $\Delta\chi \approx 10^{-6}$  in SI) and human brain. Experimental results reported here show that  $\Delta\chi$  variations are correlated with the amount of deviation from Gaussian behavior observed in diffusive decay of water in both controlled phantoms and human brains using Kurtosis approach.

3624. 65 **Comparison between kurtosis and biexponential models for diffusion-weighted brain imaging with high resolution and high b-factor**  

Bibek Dhital<sup>1</sup>, and Robert Turner<sup>1</sup>

<sup>1</sup>Max Planck Institute for Human Cognitive and Brain Sciences, Leipzig, Germany

B-factors greater than 2000 s.mm<sup>-2</sup> are rarely used in diffusion-weighted imaging, due to the consequent loss of adequate SNR. Early studies at high b-factor used biexponential fitting, but recently its appropriateness for human brain imaging has been questioned, and kurtosis analysis has been proposed as an alternative with fewer fit parameters. Benefitting from the high SNR of diffusion-weighted STEAM-EPI at 7T, we acquired diffusion-weighted images with a resolution of 2 mm isotropic and maximum b-value of 8000 s.mm<sup>-2</sup>. Comparing biexponential fits to kurtosis fits for each voxel, we found that biexponential fits showed much superior goodness-of-fit throughout the brain.

3625. 66 **USING THE CHARMED MODEL TO ELUCIDATE THE UNDERPINNINGS OF CONTRAST IN DIFFUSIONAL KURTOSIS IMAGING**  

Silvia De Santis<sup>1</sup>, Yaniv Assaf<sup>2</sup>, and Derek K Jones<sup>1</sup>

<sup>1</sup>CUBRIC, Cardiff University, Cardiff, United Kingdom, <sup>2</sup>Tel Aviv University, Tel Aviv, Israel

The CHARMED model was used to understand whether and

where DKI contrast could be explained in terms of the underlying axonal geometry, calculating K directly from the propagator used in the CHARMED model and verifying the correlation between K and the CHARMED parameters in vivo. This work demonstrates that the information contained in DKI overlaps with the information extracted by CHARMED in areas of higher intra-voxel directional coherence, while a different information content in areas of non-negligible fibre dispersion.

3626.

67

### **Multi-TE diffusion kurtosis imaging in vivo**

Alexandru Avram<sup>1</sup>, Arnaud Guidon<sup>2</sup>, Chunlei Liu<sup>3</sup>, and Allen W Song<sup>3</sup>

<sup>1</sup>*Section on Tissue Biophysics and Biomimetics, NICHD, National Institutes of Health, Bethesda, Maryland, United States,* <sup>2</sup>*Biomedical Engineering Department, Duke University, Durham, NC, United States,* <sup>3</sup>*Brain Imaging and Analysis Center, Duke University Medical Center, Durham, NC, United States*

In this report we compare in vivo diffusion kurtosis measurements acquired with short and long echo times (TE) and discuss their potential for deriving a diffusional kurtosis measures for myelin water in vivo. Our findings provide initial evidence that the apparent kurtosis coefficient vary significantly with TE indicating differences between diffusional characteristics of T2 water pools in white matter.

3627.

68

### **Accuracy of Diffusional Kurtosis Imaging in Resolving White Matter Fiber Crossings**

Ali Tabesh<sup>1</sup>, Jens H. Jensen<sup>1</sup>, and Joseph A. Helpert<sup>1,2</sup>

<sup>1</sup>*Radiology and Radiological Science, Medical University of South Carolina, Charleston, South Carolina, United States,* <sup>2</sup>*Neurosciences, Medical University of South Carolina, Charleston, South Carolina, United States*

The accuracy of diffusional kurtosis imaging (DKI) in resolving crossing fiber bundles was compared via simulations to those of diffusion spectrum imaging (DSI) and Q-ball imaging (QBI). The accuracies of these techniques and DTI were also investigated when a dominant fiber bundle intersects with an admixture of a subdominant bundle. The simulations utilized the analytical orientation distribution function representation for each technique. DSI provided the most accurate estimates in both comparisons, whereas QBI with  $b = 4000$  s/mm<sup>2</sup> and DKI with  $b = 2000$ -2500 s/mm<sup>2</sup> offered similar accuracies. Finally, DKI was superior to DTI in estimating the dominant fiber bundle direction.

3628. 69 **Power and variability analysis in diffusion kurtosis imaging: Sample size estimation in three white matter structures**  

Filip Szczepankiewicz<sup>1,2</sup>, Alexander Leemans<sup>3</sup>, Pia Sundgren<sup>1,4</sup>, Ronnie Wirestam<sup>2</sup>, Freddy Ståhlberg<sup>1,2</sup>, Danielle van Westen<sup>1,4</sup>, Jimmy Lätt<sup>4</sup>, and Markus Nilsson<sup>2</sup>

<sup>1</sup>Department of Diagnostic Radiology, Lund University, Lund, Sweden, <sup>2</sup>Department of Medical Radiation Physics, Lund University, Lund, Sweden, <sup>3</sup>University Medical Center Utrecht, Image Sciences Institute, Utrecht, Netherlands, <sup>4</sup>Center for Medical Imaging and Physiology, Skåne University Hospital, Lund, Sweden

Statistical power and variability analysis was performed using 20 sets of DKI data. The mean diffusivity (MD), fractional anisotropy (FA), mean kurtosis (MK) and radial kurtosis (RK) were determined in the cingulum, corpus callosum and corticospinal tract. Sample sizes required to detect a 10% difference with a power of 0.9 were calculated. Variability was divided into inter-subject biological differences and that arising from measurement noise. Minimum sample sizes varied across structures and metrics, but were approximately 15 for MD, FA and MK, and approximately 30 for RK. The inter-subject biological variability was the main contributor to total variability.

3629. 70 **The effect of the kurtosis on the accuracy of diffusion tensor based fiber tractography**  

Chantal M.W. Tax<sup>1</sup>, Sjoerd B. Vos<sup>1</sup>, Jelle Veraart<sup>2</sup>, Jan Sijbers<sup>2</sup>, Max A. Viergever<sup>1</sup>, and Alexander Leemans<sup>1</sup>

<sup>1</sup>Image Sciences Institute, University Medical Center Utrecht, Utrecht, Netherlands, <sup>2</sup>Visionlab, Department of Physics, University of Antwerp, Antwerp, Belgium



In addition to DTI, DKI quantifies the degree to which the diffusion is non-Gaussian and it can be used to estimate typical DTI measures more accurately but with lower precision. In this work, the difference in orientation information of the diffusion tensor was compared between DTI and DKI. There is a systematic deviation in orientation of the principle eigenvector, showing the difference in accuracy. In addition, deterministic and probabilistic fiber tracking on real diffusion MRI data confirms this difference in orientation information. In conclusion, the architectural configuration of the DKI based fiber pathways is more accurate than that of DTI.

3630. 71 **Regional values of the diffusional kurtosis in the healthy brain** 

Danielle Van Westen<sup>1,2</sup>, Markus Nilsson<sup>3</sup>, Nils Karlsson<sup>2</sup>, Mikael Johansson<sup>4</sup>, Freddy Ståhlberg<sup>2,3</sup>, Pia C Sundgren<sup>1,2</sup>, and Jimmy Lätt<sup>1</sup>

<sup>1</sup>Center for Medical Imaging and Physiology, Skane University Hospital, Lund, Sweden, <sup>2</sup>Diagnostic Radiology, Lund University, Lund, Sweden, <sup>3</sup>Department of Medical Radiation Physics, Lund University, Lund, Sweden, <sup>4</sup>Institute for Psychology, Lund University, Lund, Sweden

Regional values of the diffusional kurtosis, previously reported in a very limited number of structures, were determined in thirty-six healthy individuals in a large number of anatomically defined areas. Mean kurtosis varied from 1.38 in the splenium of the corpus callosum to 0.66 in the caudate head. Estimates in previously studied areas were well in line with those. Linear age-dependency for mean kurtosis was found in some regions, but no quadratic relationship with age, which may be due to the limited number of individuals studied.

3631. 72 **Optimal Diffusion Kurtosis Imaging for Clinical Use – Fewer diffusion weightings or diffusion directions?**    
 Jiachen Zhuo<sup>1</sup>, Jonathan Z. Simon<sup>2</sup>, and Rao P Gullapalli<sup>1</sup>  
<sup>1</sup>Diagnostic Radiology and Nuclear Medicine, University of Maryland School of Medicine, Baltimore, MD, United States, <sup>2</sup>Electrical & Computer Engineering, Biology, University of Maryland College Park, College Park, MD, United States

Diffusion kurtosis imaging (DKI) has gained much interest lately as a tool that can reveal subtle tissue microstructure changes over and beyond available from diffusion tensor imaging (DTI). The main challenge for clinical applications of DKI is the long imaging acquisition time due to the increased measurements needed to fit a more complex model (21 model parameters). Here we study the effect of diffusion weightings and diffusion directions in estimated DKI parameters to determine the optimal DKI imaging schemes within a clinically feasible image acquisition time (< 10min), and to understand the estimation variability in using these optimal DKI schemes.